Drexel University

Annual Progress Report: 2010 Formula Grant

Reporting Period

January 1, 2011 – June 30, 2011

Formula Grant Overview

The Drexel University received $1,275,294 in formula funds for the grant award period January 1, 2011 through December 31, 2012. Accomplishments for the reporting period are described below.

Research Project 1: Project Title and Purpose

Conformational Signatures of Neurotransmitter-Induced Gating and Desensitization of Nicotinic Ion Channels: A Collaborative Simulation and Experimental Approach - This project launches a new collaboration between the PI (Abrams) and Mike White (DUCOM Biochemistry) dedicated to the study of nicotinic ligand-gated ion channels (LGIC's), the key proteins that mediate synaptic transmission in higher organisms. LGIC's are targets for drugs involved in treating behavioral problems, substance addiction (certain LGIC's are the chief targets of nicotine), muscle control disorders, and pain. Our efforts here to elucidate the links between the molecular structure of LGIC's and their function form the foundation of longer-term rational drug design which would have a major, sustained impact on human health.

Anticipated Duration of Project

1/1/2011 - 12/31/2012

Project Overview

The broad objective of this project is the elucidation of structure/function relationships in ligand-gated ion channels (LGIC's). Our approach combines novel computational all-atom conformational sampling methods developed by the PI with wet-lab mutagenesis, expression, and electrophysiological characterization. For the one-year duration of the project, we aim to demonstrate the feasibility of our approach by testing an original hypothesis: LGIC desensitization to endogenous neurotransmitter is modulated by interactions between the M4 helix (Leu430) of the transmembrane domain and the cys-loop (Phe137) of the extracellular domain. Our prototype LGIC is the murine neuromuscular nicotinic acetylcholine receptor (AChR). We will first express and test wild-type and Leu430->Ser and Phe137Ser mutant AChR's. We will then conduct conformational-sampling computer simulations of AChR's aimed at expanding the basis for further site-specific mutagenesis on the M4 helix. The project will support one PhD student who already has experience with both molecular simulations and electrophysiology.

Principal Investigator

Cameron F. Abrams, PhD
Associate Professor
Drexel University
3141 Chestnut St
Philadelphia, PA 19104

Other Participating Researchers

Michael M. White, PhD – employed by Drexel University College of Medicine
Spencer Stober – employed by Drexel University

Expected Research Outcomes and Benefits

Our project aims to elucidate the role of helix M4 on activation and desensitization in acetylcholine receptors. The hypothesis that Leu430 on M4 interacts with Phe137 of the extracellular domain is important because, if correct, it provides a novel target for drugs that could modulate ion channel function, potentially leading to new therapies for neurological and neuromuscular disorders. The major outcomes of this one-year project will be the generation of a set of preliminary data sufficient for submission of an R-series application to NIH.

Summary of Research Completed

Molecular Simulations of nAChR:

Based on the all-atom model developed by Unwin (J. Mol. Biol. 2005) with docked cholesterols suggested by Brannigan et al. (PNAS 2009), we constructed an all-atom, explicitly membrane-anchored and solvated model of the *Torpedo* nAChR. Using NAMD 2.7 and the CHARMM 22/27 force-fields (for proteins/lipids, respectively), this model was subjected to 50 ns of molecular dynamics (MD) simulation using TeraGrid resources (approx. 80,000 hours) for equilibration. This trajectory was analyzed to determine its degree of equilibration and, beyond its equilibration time, it was further analyzed to discover intramolecular interactions that may be important for its function. To that end, the relaxed system was then subjected to several temperature-accelerated MD (TAMD) simulations for enhanced conformational sampling. The collective variables used in the TAMD calculations were centers of mass of groupings of 4-6 residues along the protein chains. Focusing on the interface between the extracellular domain (ECD) and the membrane-spanning domain (MSD), we observed that a bottleneck in this channel closing seemed to involve breakup of a set of hydrophobic interactions between the M4 helix and the cys-loop of the ECD. In particular, side-chains of Leu430 in M4 and Phe137 in the cys-loop formed the core of a hydrophobic interaction network that was destroyed during channel closure under TAMD. This interaction was seen to "flicker" on and off under normal MD. This is potentially significant because it suggests that the rate at which a channel returns to a resting state after losing its bound neurotransmitter (acetylcholine [ACh]) or the rate at which it desensitizes (closes) while ACh is still bound might be controlled by this interaction. A second

interaction that was noted from all TAMD simulations was a "ratcheting" of the top of the M2-M3 loop (Pro272) through a groove formed by residues in the b1-b2 loop (Glu45 and Val46) pulling the M2 helix away from the central axis of the pore.

Mutagenesis and Whole-cell Electrophysiology of nAChR M4 mutants:

Mutations in the α subunit of the mouse muscle AChR were created using the QuikChange Mutagenesis kit (Stratagene), and mutations were verified by sequencing. Capped messenger RNAs for the wild-type α, β, δ, and ε subunits and the αL430A and αL430V mutant subunits were synthesized *in vitro* using the mMessage Machine SP6 transcription kit (Ambion). mRNAs coding for the β, δ, and ε subunits were mixed with either wild-type or mutant α subunit mRNAs and injected into the cytoplasm of *Xenopus* oocytes, a widely-used system for the expression of ion channels and receptors. Forty-eight hours post-injection, the wild-type or mutant AChRs were studied using a two-electrode voltage clamp.

The figure below shows the response to bath application of 30 μM ACh to a voltage-clamped oocyte held at -60 mV expressing wild-type AChRs (left panel) and αL430A-containing AChRs (right panel). In both cases the traces show an inward current (downward deflection) as the receptors activate and then a slower decrease (returning towards baseline) as the receptors desensitize. All three types of receptors (wild-type, αL430A, αL430V) have essentially similar kinetics of activation and desensitization, and the dose-response curves are identical (data not shown). Thus, at first glance it appears that neither mutation affected channel opening or desensitization.

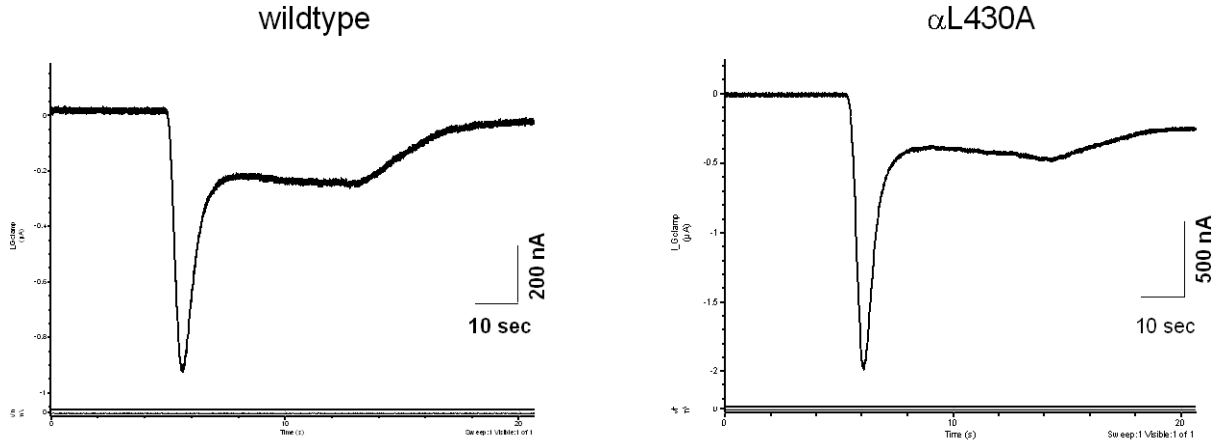

Research Project 2: Project Title and Purpose

Ischemic Injury and Neuroprotection in Newborn Piglet Brain - The objective of this research plan is to develop an in-depth understanding of the events that protect neurons from perinatal hypoxia-ischemia. At present, there are no therapies available to protect the infant brain from perinatal insults. One of the strategies of neuroprotection is neuronal hypoxic preconditioning (PC). PC provides a potential route for prophylactic intervention in patients in whom ischemic events are anticipated, such as those undergoing brain and heart surgery and those with transient

ischemic attacks. We will elucidate a novel signaling pathway leading to neuroprotection by PC induced vascular endothelial growth factor (VEGF) and its receptor activation. These studies will demonstrate a key role for VEGF in facilitating neuroprotective processes and will determine the downstream signaling intermediates that suppress cell death and promote survival during hypoxia-ischemia following PC.

Anticipated Duration of Project

1/1/2011 - 12/31/2012

Project Overview

Perinatal hypoxic-ischemic (HI) brain injury is a major cause of morbidity and mortality, often leading to learning disabilities, cerebral palsy, epilepsy and death. Effective treatment strategies are currently limited. Understanding the mechanisms underlying the phenomenon of ischemic tolerance in brain, in which brief hypoxic preconditioning (PC) confers potent neuroprotection against subsequent HI injury, may yield powerful insights into both the control of cell death and therapeutic strategies with which to treat HI brain injury. Hypoxia has been shown to be a potent inducer of vascular endothelial growth factor (VEGF) through the transcription factor hypoxia inducible factor-1 alpha (HIF-1α). However, the signal transduction pathways mediating the neuroprotective effects of VEGF are not fully understood. Our goal is to determine the molecular mechanisms of PC-induced VEGF signaling pathways in protecting newborn brain against HI injury. We hypothesize that PC will elicit tolerance to subsequent HI in newborn piglets by blocking caspase-independent neuronal death via VEGF-VEGF receptor mediated activation of cyclic AMP responsive element binding protein (CREB) pathways. We have developed a newborn piglet model of induced tolerance to cerebral hypoxia-ischemia. Using newborn piglet model of induced tolerance to cerebral HI, we propose to: 1) determine whether PC-induced activation of VEGF/VEGF receptors in newborn piglet brain results in protection of HI-induced brain damage. We will selectively knockdown VEGFR1 and VEGFR2 receptor activity immediately after PC using pharmacological inhibitors and small interfering RNA's (siRNA's) *in vivo* to determine whether inhibition of their expression abolishes VEGF-induced tolerance to cerebral HI following preconditioning. 2) To determine whether VEGF activates CREB pathways via signaling through VEGFR1 and VEGFR2 to induce neuroprotection in hypoxic preconditioned newborn brain. We will assess the phosphorylation state of CREB at Ser^{133} before and after treatment with VEGF receptor inhibitors and siRNA's following PC to determine its involvement in VEGF/VEGF receptor mediated neuroprotection. We will also test specific kinases especially MAPK, PI3K/AKT and GSK3β that mediate CREB phosphorylation downstream of VEGF to determine the importance of these pathways to HI tolerance. The proposed studies will identify the specific molecular mechanisms of neuroprotective actions of VEGF against hypoxic-ischemic injury in the brain and will contribute to the development of novel therapeutic and/or preventive strategies for treating HI neonatal brain injury.

Principal Investigator

Jahan Ara, PhD
Assistant Professor
Drexel University College of Medicine
245 N. 15th Street
MS 1029
Philadelphia, PA 19102

Other Participating Researchers

Francis Kralick, DO - employed by Hahnemann University Hospital
Jason Ohlstein, MS - employed by Drexel University College of Medicine

Expected Research Outcomes and Benefits

An innovative feature of our project is that it will elucidate a novel signaling pathway leading to neuroprotection by preconditioning induced VEGF/VEGF receptor activation primarily acting through cyclic AMP responsive element binding protein (CREB). These results will be significant because they will demonstrate a key role for each of the VEGF receptors, in facilitating neuroprotective processes and will determine the downstream signaling intermediates that suppress cell death and promote survival during hypoxia-ischemia following hypoxic preconditioning. Our preliminary studies strongly indicate that programmed cell death mediated by apoptosis-inducing factor (AIF) can also occur in the complete absence of caspase activation and that preconditioning prevents AIF translocation into the nucleus after hypoxic-ischemic insult. This research project will generate data to demonstrate a key role for AIF in delayed neuronal cell death after hypoxia/ischemia insults *in vivo* and will provide a link between enhanced CREB activation and prevention of mitochondrial AIF release and caspase-independent execution of neuronal cell death in our tolerant model.

Summary of Research Completed

Data from specific aim 1:
Silencing of VEGFR1 and VEGFR2: For the past three months we have been working on inhibiting VEGF receptors to define the effects of blocking VEGF receptors on neuroprotection in neonatal piglet brain. To characterize the effects of VEGFR1 and VEGFR2 inhibitors on VEGFR1 and VEGFR2 mRNA expression as well as on VEGFR1 and VEGFR2 phosphorylation, we used VEGFR1 and VEGFR2 inhibitors *in vivo* and *in vitro*, and also RNA-mediated interference (RNAi) against VEGFR1 and VEGFR2 *in vitro*. For *in vitro* studies, we used neural stem/progenitor (NSP) cell cultures derived from subventricular zone (SVZ) of newborn piglet brain.

For *in vitro* siRNA transfection, Stealth RNAi siRNA duplex oligoribonucleotides that were targeting human VEGFR1 and VEGFR2 were purchased from Invitrogen. The sequences of the two duplexes used for VEGFR1 and VEGFR2 silencing are listed in Table 1. Neural stem/progenitor cells were transfected with 25 nM or 50 nM control or Stealth siRNA duplexes

targeting VEGFR1 and VEGFR2 and 2 µL of Lipofectamine™ RNAiMAX (Invitrogen). After transfection for 72h, cells were harvested for quantitative PCR analysis. Differentiated NSPs were also treated with either vehicle (DMSO) or VEGFR2 inhibitor SU1498 (10 µM -50 µM) for 1h and then stimulated with 50ng/ml VEGF for 15 minutes. Cells were harvested for quantitative polymerase chain reaction (PCR) and Western blot analysis.

The analysis of cellular mRNA levels by quantitative PCR revealed a profound approximately 87% down-regulation of VEGFR1 mRNA levels 72h after treatment with either 25 nM or 50 nM stealth VEGFR1 siRNA (Figure 1A). This effect was not associated with any visible signs of toxicity. The treatment with either 25nM or 50nM stealth VEGFR2 siRNA did not change the mRNA expression of VEGFR1 (Figure 1A).

The quantitative real-time PCR analysis of VEGFR2 showed that mRNA of this receptor was down-regulated in the NSP cells derived from newborn piglet SVZ by treatment with stealth VEGFR2 siRNA. The expression level of VEGFR2 mRNA decreased by 72% at 72h after treatment with 25 nM and by 80% after treatment with 50 nM stealth VEGFR2 siRNA (Figure 1B). VEGFR1 stealth siRNA had no effect on the mRNA expression of VEGFR2 at either of the concentrations (Figure 1B). Currently we are working out the conditions to perform *in vivo* siRNA transfer.

Pretreatment of NSP cells with VEGFR2 inhibitor SU1498 (10-50µM) for 1h inhibited the mRNA expression of VEGFR2 in a dose dependent manner. The quantitative PCR analysis showed that the expression of VEGFR2 mRNA decreased by ~2 fold at 25 µM and by 5 fold at 50 µM SU1498 compared to untreated controls. An interesting finding of this study was that VEGFR1 mRNA expression in NSP cells treated with SU1498 increased in a dose-dependent manner as shown in Figure 2.

To examine the effect of VEGFR2 receptor inhibition *in vivo*, VEGFR2 inhibitor SU1498 was used. One-day-old piglets were subjected to preconditioning ($8\%O_2/92\%N_2$) for 3h. Immediately after preconditioning, animals received DMSO or DMSO containing SU1498 (10-25mg/kg body weight) using cisternal tap. The animals were subjected to severe hypoxia-ischemia (5% FiO_2 for pre-defined period of 30 minutes, and ischemia induced by a period of hypotension -10 minutes of mean arterial blood pressure reduced to $\leq$ 70% of baseline) and recovered for 24 and 48h, and brains were harvested for Western blot analysis. Addition of SU1498 abrogated VEGF induced VEGFR2 phosphorylation at 24 and 48h (Figure 3).

Data from specific aim 2:
Hypoxic-preconditioning prevents AIF translocation in newborn piglet brain: We examined the subcellular distribution of AIF in hypoxic-ischemic (HI) and preconditioning+hypoxic-ischemic (PC+HI) animals by Western blotting and immunofluorescence. Western blot analysis of the nuclear fraction of HI brain samples revealed a significant elevation of translocated nuclear AIF levels. In the normoxic brain, AIF was present exclusively in the mitochondria (Figure 4A). AIF translocation to the nucleus from mitochondria occurred as early as 0h after HI and significantly increased at 24h and 3 days after HI compared to normoxic controls (Figure 4B). On the other hand, preconditioning performed 24h prior to severe HI attenuated AIF translocation into the nuclear fraction (Figure 4B) as reflected by reduced nuclear AIF expression.

To ascertain whether HI could induce caspase-mediated cell death, activation of caspase-3 was examined in HI and normoxic brains by Western blotting using antibodies that recognize both active and inactive forms of caspase-3. Western blotting (Figure 4C) revealed that the caspase-3 was clearly not activated in HI newborn piglet brain suggesting that HI induced cell death is independent of caspase cascade.

We next analyzed the cellular distribution of AIF by immunohistochemistry in brain sections obtained at 24h and 3 days after HI and PC+HI. In normal brains, AIF showed clearly extranuclear, i.e., cytoplasmic staining (Figure 5) that colocalized with COX (cytochrome c oxidase subunit IV), a mitochondrial marker. In sections from HI brains at 3 days of recovery, a large number of cells in the cortex (Figure 5) showed AIF immunofluorescence with a nuclear localization (co-staining with Hoechst), confirming the nuclear translocation of AIF. In contrast, the occurrence of cells with nuclear AIF translocation was greatly decreased in PC+HI newborn brains compared to HI brains (Figure 5).

Hypoxic preconditioning activates GSK-3β and CREB in newborn piglet brain: We investigated the cytoplasmic signaling pathways activated by preconditioning and investigated the pathways through which cytoplasmic signaling transmits signals into the nucleus. Our data demonstrated that preconditioning significantly phosphorylated and inhibited GSK-3β in the cytosol and activated CREB in nucleus. As shown in Figure 6, preconditioning caused an increase in phosphorylation of GSK-3β in cytosolic extracts of piglet brain at 24h and 3 days of recovery compared to controls. Densitometric analysis showed that p-GSK-3β levels were 1.5 and 2 fold higher at 24h and 3 days of recovery, respectively.

Western blots prepared from nuclear extracts of cortex of normoxic and PC animals were probed with an antibody directed toward CREB phosphorylated on Ser^{133}. Exposure of newborn piglets to PC followed by 24h, 3 and 7 days of recovery resulted in 2 fold (at 24h) and 4 and 5 fold (at 3 and 7 days) increase in p-CREB expression compared to controls (Fig. 7A). Phosphorylated CREB levels were also measured at 0h, 24h and 3 days in HI and PC+HI piglets in nuclear extracts after reoxygenation. Densitometric analysis showed that p-CREB levels were 1.5 fold greater at 0h and 24h and 3 fold greater at 3 days in animals that were preconditioned 24h prior to HI compared to animals that were subjected to HI alone (Fig. 7B).

TABLE 1

Gene Name	RNA name	Sequence 5′-3′
VEGFR1	EU714325-A	CAGCUUUACACGUGGAGCCUAAGAA
VEGFR1	EU714325-A	UUCUUAGGCUCCACGUGUAAAGCUG
VEGFR1	EU714325-C	CAGAUUCACGUGGAGUCCAACUGAA
VEGFR1	EU714325-C	UUCAGUUGGACUCCACGUGAAUCUG
VEGFR1	EU714325-B	CAGAUCAUGUUGGACUGUUGGCACA
VEGFR1	EU714325-B	UGUGCCAACAGUCCAACAUGAUCUG
VEGFR2	EU714326-A	CCAAGUGAUUGAAGCAGAUGCCUUU
VEGFR2	EU714326-A	AAAGGCAUCUGCUUCAAUCACUUGG
VEGFR2	EU714326-C	CCAUAGUAAGUGACGCGUACGAUUU
VEGFR2	EU714326-C	AAAUCGUACGCGUCACUUACUAUGG
VEGFR2	EU714326-B	AAGGAGAUGCUCGCCUCCCUUUGAA
VEGFR2	EU714326-B	UUCAAAGGGAGGCGAGCAUCUCCUU

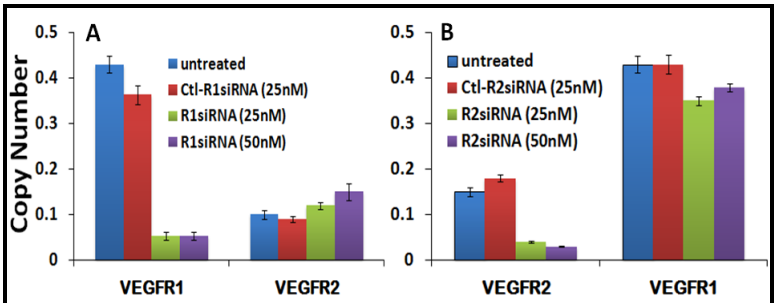

Fig. 1: VEGFR1 and VEGFR2 mRNA expression in neural stem/progenitor cells treated with Stealth RNAi siRNA duplexes

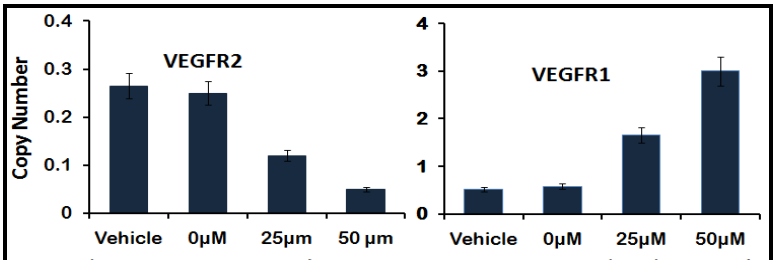

Fig. 2: VEGFR2 and VEGFR1 mRNA expression in neural stem/progenitor cells treated with VEGFR2 inhibitor SU1498. SU1498 inhibited the mRNA expression of VEGFR2 in a dose dependent manner.

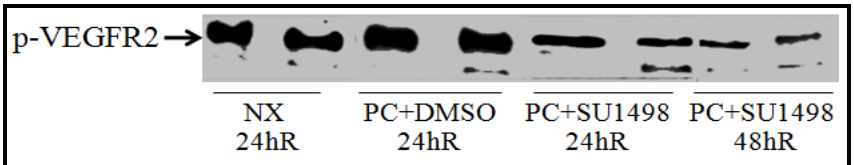

Fig. 3: Western blot analysis showing VEGFR2 phosphorylation in SU1498 and DMSO treated animals at 24 and 48h recovery. Addition of SU1498, inhibited VEGF induced VEGFR2 phosphorylation at 24 and 48h.

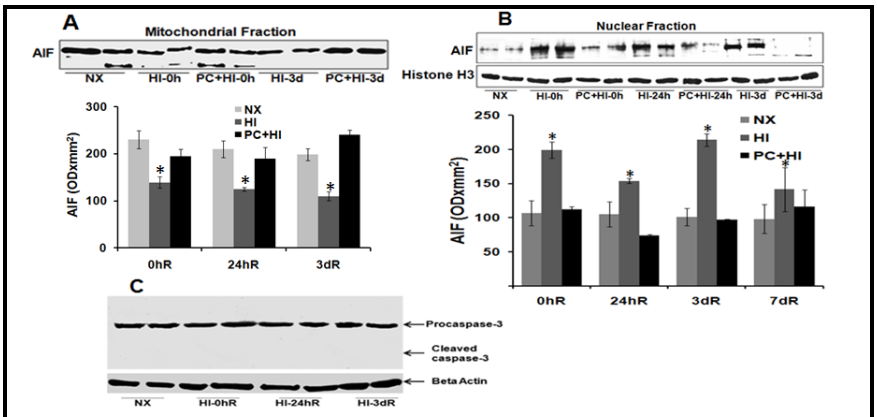

Fig. 4: (A) Western blotting showing AIF in mitochondrial fraction of NX, HI and PC+HI animals. (B) Western blotting reveals an increase in AIF in response to HI and its significant attenuation by preconditioning. Quantification of immunoblot data on AIF expression in mitochondria and nucleus by densitometric analysis shows mean ± SD of three independent experiments (*P <0.05). (C) Western blotting shows that the caspase-3 is not activated in HI newborn piglet brain.

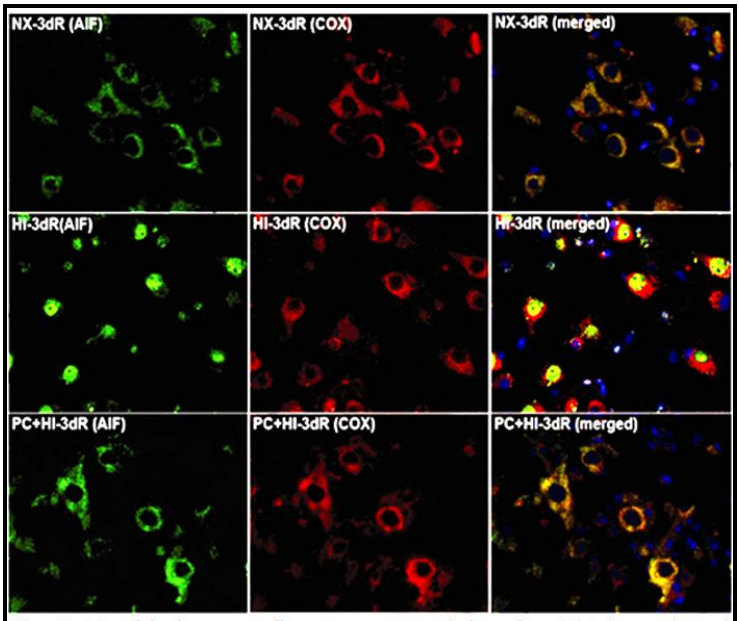

Fig. 5: Double immunofluorescence staining for AIF (green) and COX (red) in normoxic, HI and PC+HI cortex. AIF/COX merged cells in NX and PC+HI brain are shown as yellow. In HI brain AIF shows nuclear localization (costaining with Hoechst).

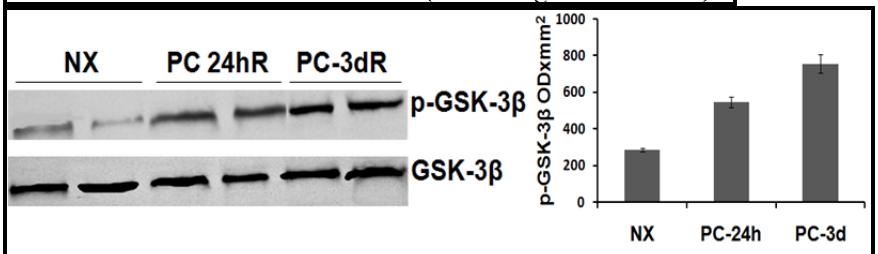

Fig. 6: Representative immunoblots of p-GSK-3β, and GSK-3β from cytosolic extracts of cortex of NX and PC piglets. Data represent mean ± SD (n=6).

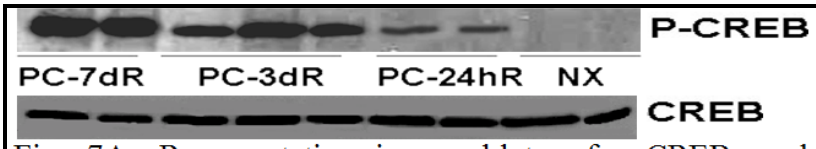

Fig. 7A: Representative immunoblots of p-CREB, and CREB from nuclear extracts of cortex of NX and PC piglets. Data represent mean ± SD (n=6).

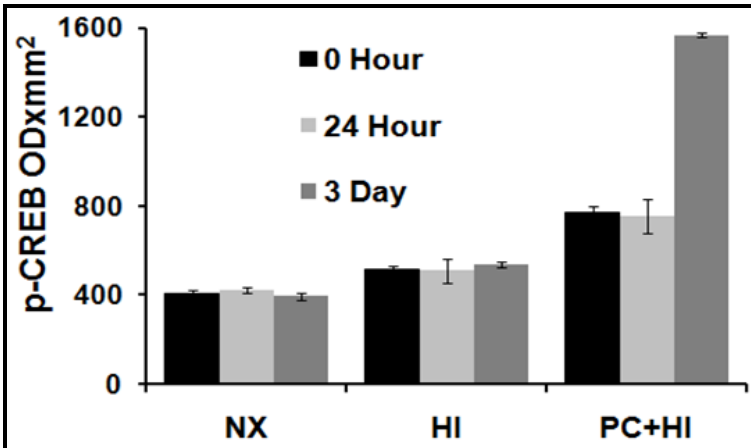

Fig. 7B: Quantification of immunoblot data on p-CREB expression by densitometric analysis. Data represent means ± SD of 3 independent experiments. $P < 0.05$.

Research Project 3: Project Title and Purpose

Targeted Gene Delivery for Treatment of Cardiomyopathy in Muscular Dystrophy - The purpose of the project is to develop methodologies to deliver genes into the heart muscle cells safely and effectively to treat cardiomyopathy. These studies will assess the feasibility, safety and efficacy of gene delivery to restore myocardial structure and function. We also anticipate investigating the mechanisms of action and optimization of strategies of these methodologies.

Anticipated Duration of Project

1/1/2011 - 12/31/2012

Project Overview

In this project, we will pursue the hypothesis that gene therapy can restore myocardial structure and function. We will test this hypothesis by 4 specific aims:

1. To develop: 1) micro-bubbles; 2) green florescence protein (GFP) reporter system; and 3) DNA plasmid for *in vitro* and *in vivo* gene delivery experiments.

2. To optimize the efficiency of delivery of GFP reporter gene complex using cultured murine myocytes and micro-bubble targeted methodologies.
3. To pursue the efficacy and safety of modified gene therapy for *in vivo* delivery using mouse models and micro-bubble targeted methodologies.
4. A final set of experiments will investigate myocardial structure and function by these methodologies and strategies to treat cardiomyopathy in mouse models.

Our experimental designs are as follows:

1. Chemistry and in vitro experiments
DNA loading onto the micro-bubbles. Optimized DNA-loaded micro-bubble will be tested in vitro by contacting them with myocytes grown to 80% confluence in Opticell cassettes. After 24 hours, cells will be checked for GFP (fluorescent microscope). Optimized procedures will be finally tested with the gene complex.

2. *In vivo* animal studies
Loaded micro-bubbles will be injected into the tail veins of anesthetized mice at 9 months. The animals will be studied by histology, molecular and cell assays for mechanism of action, safety and efficacy. Gene delivery efficiencies will be assessed by measuring GFP expression by fluorescence studies. Longitudinal follow-up studies will also be conducted by microscopy before and after treatment as well as weekly x 4 weeks for structural and functional alterations.

Principal Investigator

Shuping Ge, MD
Associate Professor of Pediatrics
St Christopher's Hospital for Children
3601 A Street
Philadelphia, PA 19134

Other Participating Researchers

Margaret A. Wheatley, PhD – employed by Drexel University
Xiongwen Chen, PhD – employed by Temple University

Expected Research Outcomes and Benefits

These studies will provide the first preliminary data to assess the feasibility, safety and efficacy of gene delivery to restore myocardial structure and function. We also anticipate investigating the mechanisms of action and optimization of strategies of these methodologies. These data will provide the rationale to design in depth experiments to rigorously evaluate these methodologies in *in vitro* and *in vivo* experiments by securing external funding. The ultimate goal is that scientific discoveries and opportunities from these studies will be further validated and translated into clinical trials to search for a cure for this lethal disease.

Summary of Research Completed

Aim 1. To develop: 1) micro-bubbles; 2) green florescence protein (GFP) reporter system; and 3) DNA plasmid for *in vitro* and *in vivo* gene delivery experiments.

Experiment 1. Microcapsules were prepared by an adapted double emulsion (W/O)/W solvent evaporation process. Camphor (0.05 g) and poly (lactide acid) PLA (0.5 g) were dissolved in 10 mL of methylene chloride, and 1.0 mL of deionized water containing ammonium carbonate (0.04g/ml) was added and the polymer solution was probe sonicated at 110 W for 30 s. The resulting emulsion was then poured into a cold (4°C), 5% polyvinyl alcohol solution and homogenized for 5 min at 9500 rpm. The double emulsion (W/O)/W was then poured into a 2% isopropanol solution and stirred at room temperature for 1 h, to evaporate off the methylene chloride, and thus dry the capsules. The capsules were collected by centrifugation, washed one time with deionized water, centrifuged (at 15°C for 5 min at 5000g), and the supernatant was discarded. The capsules were then washed three times with hexane to further extract the methylene chloride. The capsules were frozen in a -85°C freezer and lyophilized, using a Virtis Benchtop freeze dryer. Camphor and water sublime when freeze dried, leaving a void in their place and producing hollow PLA microcapsules.

Experiment 2. Hearts were removed from neonatal rats, vessel, atria and connective tissues were trimmed away, and hearts were transferred into a sterile 30 ml beaker. Digestion buffer was added, stirred in an oven (at 37°C for 12min) and spun at 1200 rpm for 1min. The isolated pelleted cells were resuspended in culture medium. Cell were plated on three uncoated 100mm plates for 1-2h at 37°C to reduce the contamination of cardiac fibroblasts. One hour later, the unattached cells were plated onto Opticell plates.

Aim 2. To optimize the efficiency of delivery of GFP reporter gene complex using cultured murine myocytes and micro-bubble targeted methodologies.

Experiment 1. Left ventricular cardiomyocytes from neonatal rats were cultured in 6-well plates. The growth medium was removed and replaced with 1.5 ml of fresh growth media (DMEM) containing 10% FBS, plasmid DNA for GFP (10µg DNA/ml) and polymer microbubbles (2 µm in diameter) with concentrations of (0.0, 0.025, 0.1 or 0.5 mg/ml). A 1 MHz portable ultrasound physiotherapy machine (Sylvan Inc) was coupled to the bottom of the culture plate with ultrasound gel and used to insonate cells for 10 seconds with intensity = 2.3 W/cm^2, pulse length (PL) = 5 ms, and pulse repetition rate (PRF) = 150 Hz. After insonation, cells were placed in the incubator for 4 hours, then the media was replaced with fresh media containing 10% FBS and antibiotics. After 24 and 48 hours, cells were imaged with a fluorescent microscope.

Experiment 2. Left ventricular cardiomyocytes from neonatal rats were cultured in Opticell cassettes. The growth medium was removed and replaced with fresh growth media (RPMI 1640 or DMEM) containing 10% FBS, 0.25 mg/ml polymer microbubbles (2 µml) and plasmid DNA containing the gene for GFP (10µg DNA/ml). Opticells were placed in a water bath (37°C) with a 2.25 MHz spherically focused transducer (Panametrics) oriented perpendicular to the Opticell, 45 mm from the surface. The transducer was triggered with a function generator through a RF amplifier (55 dB) with a pulse length (PL) of 20 µs, a pulse repetition frequency (PRF) of 3000

Hz, and peak negative pressures of 0.0 MPa, 0.30 MPa, 1.64 MPa, or 4.3 MPa. After insonation for 15 seconds, the Opticells were then placed in an incubator for 4 hours. The media was then removed and replaced with fresh media containing 10% FBS and antibiotics. The cells were then imaged with a fluorescent microscope at 24 and 48 hours.

GFP transfection is feasible using both approaches (Figure 1). Transfection efficiency is related to the carrying apparatus and media (data not shown). There is an ultrasound intensity dose-effect relationship, as shown in Figure 1.

Work is in progress to quantify GFP expression.

These results showed the feasibility and efficiency of in vitro reporter gene transfection to murine left ventricular cardiomyocytes. Further optimization will be done to facilitate *in vivo* experiments as proposed in Aim 3 and 4.

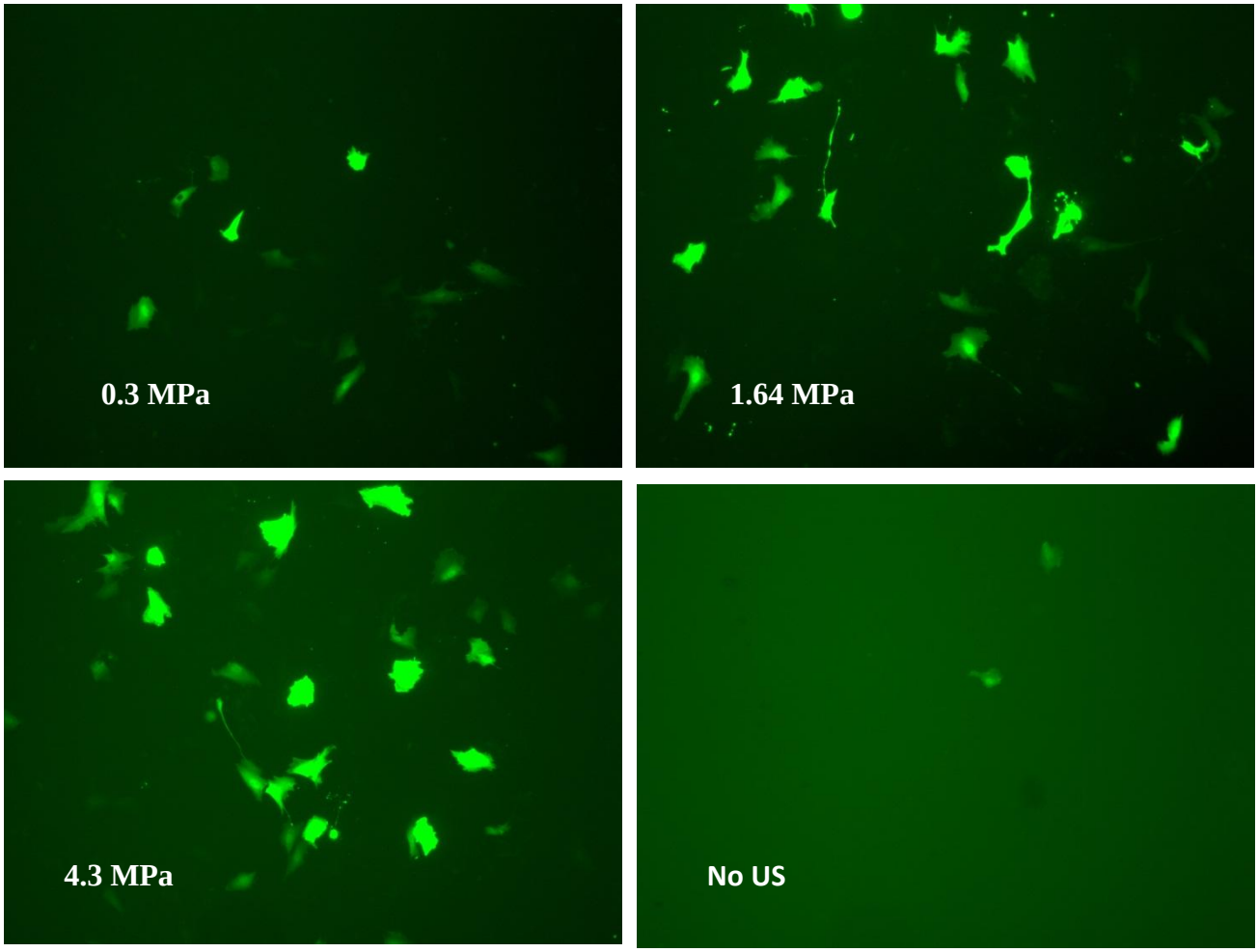

Figure 1 Transfection of GFP using ultrasound targeted microbubble destruction. DMEM Group.

Research Project 4: Project Title and Purpose

Improving the Epidemiology of Alcohol-Related Violence and Morbidity in the City of Philadelphia - The goal of this project is to use geographic information systems (GIS), spatial analysis and advanced statistical techniques to improve epidemiological studies of alcohol-related violence and injuries in the city of Philadelphia.

Anticipated Duration of Project

1/1/2011 - 12/31/2012

Project Overview

For our project, we propose a very specific set of substantive and methodological goals. Substantively, we wish to address how type of alcohol outlet, neighborhood social cohesion, and land use interact to influence rates of neighborhood violence in Philadelphia.

The specific questions this research seeks to address include: 1) Is the density of alcohol outlets in Philadelphia associated with neighborhood levels of violence? 2) Does violence geographically and temporally cluster around alcohol outlets? 3) How quickly does this association decay with time and distance? 4) Is the association between alcohol outlets and violence moderated by neighborhood cohesion or by types of land use in the area? 5) Do the spatial and temporal methodologies employed in prior research accurately capture the complexities of urban environments for helping explain violence?

From a methodological perspective, an important aspect of our proposed research is combining purely exploratory methods – such as geovisualization using GIS and map based graphics and spatial data mining – with confirmatory methods like Bayesian hierarchical regression, local and global autocorrelation, and clustering. This is all oriented toward developing and testing hypotheses about urban spatial structure and neighborhood social disorganization as they relate to alcohol and violence.

Principal Investigator

Anthony H. Grubesic, PhD
Associate Professor
Drexel University
3141 Chestnut St.
Philadelphia, PA 19104

Other Participating Researchers

Loni Philip Tabb, PhD – employed by Drexel University

Expected Research Outcomes and Benefits

This project will create several tangible results. Most important is the scientific contribution we will make by answering our outlined research questions. Given our interdisciplinary approach, these findings promise to be of interest to a broad range of disciplines, including geography, epidemiology, biostatistics, criminology, public health, urban planning and sociology. Second, it is likely that this work will help contribute to an increased awareness of alcohol-related violence at the neighborhood level in Philadelphia. As a result, local businesses, their surrounding communities and policymakers will be equipped with rigorous empirical evidence to begin the process of addressing liquor permitting issues. This might be accomplished by setting thresholds on their density, limiting outlets in high risk areas or proposing the closure of outlets that have proven to be a public nuisance by repeatedly violating liquor laws or being a hot spot for crime. Third, the project will also create several tangible results that will aid us in securing external support. During the one-year timeline of our project, members of our team will present the results of our different analyses at four important venues: (1) APHA (American Public Health Association Annual Meeting), (2) Joint Statistical Meetings (American Statistical Association), (3) URISA (Urban and Regional Information Systems Association) GIS in Public Health Conference and (4) AAG (Association of American Geographers Annual Meeting). As these papers are completed they will be submitted for publication to leading journals in multiple disciplines. All these products will serve as the basis for a grant proposal for an expanded project that will include one or two more large cities in the Commonwealth of Pennsylvania. Further, this future proposal will apply what we have learned from this project to more outcomes (e.g., calls for service, alcohol-related accidents, DUIs, alcohol-related admissions to emergency rooms, etc.).

Summary of Research Completed

PI Grubesic and Co-PI Tabb began work on this project in early January 2011. As outlined in the submitted proposal, our initial research goals during the first quarter of research (January – April) were to collect, tabulate and prepare aggravated assault data (via the Philadelphia Police Department) and alcohol outlet data (via the Pennsylvania Liquor Control Board) for the city of Philadelphia. In sum, nearly 9,000 aggravated assaults and 2,000 alcohol outlets for the year 2010 were assigned geographic coordinates (latitude and longitude) and readied for visualization in a geographic information system. There were several challenges during this phase of the research project. Most notably, many of the address records for the crime data and alcohol outlets required cleansing. For example, some of the records were missing street suffixes (e.g. ST., CT., BLVD, etc.). Further, there were numerous records where street names were misspelled, incomplete or incorrect. As a result, all assault and alcohol outlet data were cleansed and cross-referenced with parcel database for the city of Philadelphia to ensure that the final geographic coordinates were as accurate as possible. Needless to say, this is a time-consuming endeavor, but critical to generating robust and reliable exploratory and confirmatory analysis.

While data for Philadelphia were being processed by PI Grubesic and Co-PI Tabb, Grubesic and Pridemore (a consultant on the project), submitted, revised and published a paper which served

as a methodological proof of concept for testing the spatial relationships between alcohol outlets and violence.

Grubesic, T.H. and W.A. Pridemore. (2011). Alcohol Outlets and Clusters of Violence. *International Journal of Health Geographics*. 10:30.

URL: http://www.ij-healthgeographics.com/content/10/1/30

The results of the statistical analysis for Cincinnati suggest that while alcohol outlets are not problematic per se, assaultive violence has a propensity to cluster around agglomerations of alcohol outlets. This spatial relationship varies by distance and is also related to the characteristics of the alcohol outlet agglomeration. Specifically, spatially dense distributions of outlets appear to be more prone to clusters of assaultive violence when compared to agglomerations with a lower density of outlets.

Although this was a slight deviation from the proposed research plan, it proved to be a good one. There are two reasons for this. First, it allowed our research team to leverage an existing, "ready-to-go" database of assaults and alcohol outlets for the city of Cincinnati to refine and test our proposed methodologies. Second, it sets the stage for a comparative analysis between two major urban locales, Philadelphia and Cincinnati, adding supplementary perspective to the impacts of alcohol outlets and violence outside of our primary study area (Philadelphia). In the end, we anticipate that this will also allow for more meaningful and generalizable interpretation of public policy relating to violence and alcohol-related morbidity.

Results of this analysis were disseminated at a major international conference (Annual Meeting of the Association of American Geographers) in Seattle, WA during April by PI Grubesic.

During our second quarter of research, May – August, we had planned to integrate a student research assistant into the project. However, because the funds were so late in arriving to Drexel (5/24/11), our student prospects were forced to accept positions elsewhere. We hope to have a student participating during the Autumn quarter of 2011.

During the month of May, all three team members drafted and submitted a second research article, "Alcohol Outlets and Assaultive Violence in Philadelphia" to *Social Science and Medicine*, a major international, peer reviewed journal. In this paper, we enhanced the methodological approaches utilized for the previously mentioned *IJHG* article and explored the spatial linkages between alcohol outlets and the distribution of assaultive violence in the city of Philadelphia. Using a combination of exploratory spatial data analysis (ESDA) methods, we found clusters of assaultive violence around alcohol outlets and were able to determine the distances of these clusters from outlet agglomerations. Further, the team developed a new visualization approach to explore how these agglomerations interact, hypothesizing that outlet proximal agglomerations may be creating a multiplicative effect on violence. Figure 1, which is attached to the end of this section, highlights statistically significant distance ranges (colored bands), where the observed number of assaults exceed the expected number for several neighborhoods in Philadelphia. Specifically, thicker bands correspond to a larger distance range where observed assaults exceed the expected distribution. For example, the second distance

band for Agglomeration 9 is the largest in the analysis, extending from 1,031 ft. to 1,505 ft. Of particular interest are the locations where bands intersect in the study area. For example, both the first and second bands for Agglomeration 6 and Agglomeration 7 intersect. While individual assaults are not explicitly assigned to each outlet agglomeration, the geographic proximity of assault clusters and their associated overlaps may represent particularly problematic or dangerous places in Philadelphia, at least where alcohol-related assaultive violence is concerned.

Results of this analysis were disseminated at the URISA GIS and Public Health Conference in Atlanta, GA during June by PI Grubesic.

(http://www.urisa.org/files/PH%20Final%20Program.pdf)

Finally, the team is currently conducting research and beginning to draft a third paper that incorporates Bayesian disease mapping for highlighting how distribution of alcohol outlets as well as the local ecological characteristics (e.g., demographic, socio-economic, land use, etc.) of Philadelphia neighborhoods impact violence. Current research challenges include defining the appropriate spatial structures and rules for incorporating local geographic context into the statistical analysis and the development of realistic and parsimonious model structures to best reflect the connections between alcohol outlets, violence and neighborhood structures. In addition, we are also developing an alternative spatial scan statistic to detect clusters of violence.

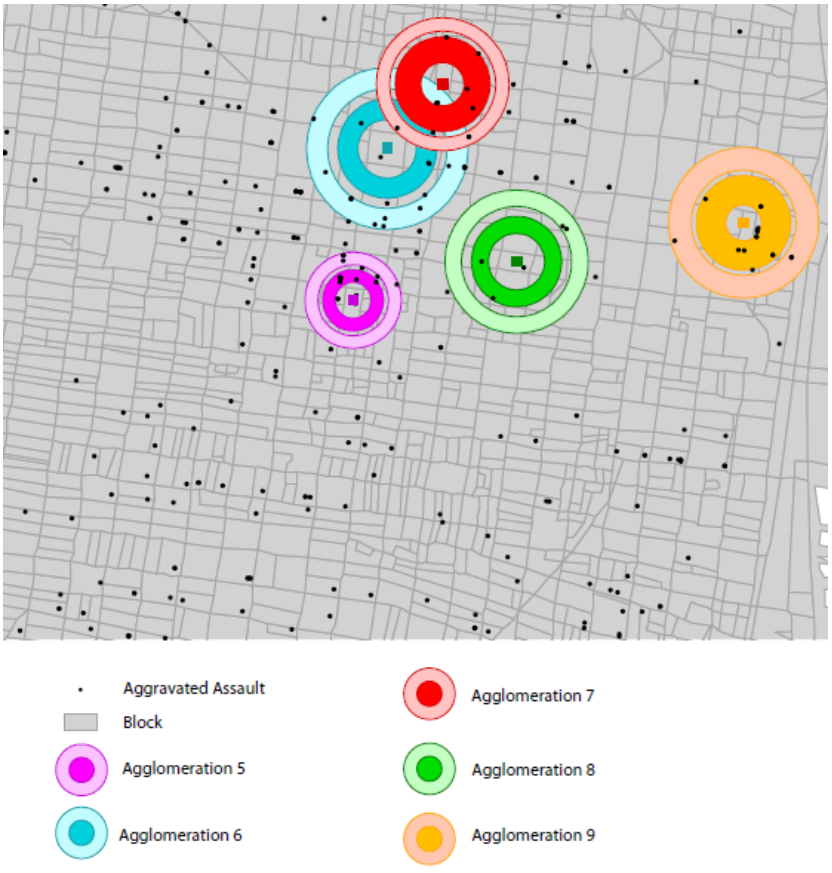

Figure 1: Alcohol Outlet Agglomerations and Violence: Statistically Significant Distance Bands

Research Project 5: Project Title and Purpose

Identification of Genetic Modifiers in a Transgenic Model of Amyotrophic Lateral Sclerosis (ALS) - Amyotrophic Lateral Sclerosis is a neurodegenerative disease leading to death in 2-5 years. Ten percent of all cases are familial; of these, 20% are caused by a mutation in the SOD1 gene. Transgenic (Tg) mice possessing the human G93A SOD1 gene also develop ALS. However, mice of the C57Bl6 strain carrying the Tg live significantly longer than do SJL mice. We have identified a Quantitative Trait Locus on the mouse Chromosome (Chr) 17 that is strongly linked to this difference in survival. The overall goal of this project is to identify genes within Chr 17 that influence longevity in this ALS model. Identification of the responsible gene(s) will highlight cellular pathways involved in motor neuron degeneration and provide new targets for the development of therapeutics to slow or stop the progression of ALS.

Anticipated Duration of Project

1/1/2011 - 12/31/2012

Project Overview

Amyotrophic Lateral Sclerosis (ALS) is a progressive disorder of the motor system leading to death within two to five years. Although most cases of ALS are sporadic in origin, 10-15% are inherited. Among the population with familial ALS, 15-20% possess a mutation in the SOD1 gene that codes for the enzyme Cu/Zn superoxide dismutase. Transgenic (Tg+) mice expressing a mutated human SOD1 gene (G93A) demonstrate clinical symptoms and neuropathological findings similar to human ALS. We have previously demonstrated that genetic background and gender affect disease phenotype in transgenic mice expressing the mutated human or mouse SOD1. We have identified a Quantitative Trait Locus (QTL) on chromosome (Chr) 17 that is strongly linked to survival in the B6 and SJL mouse strains. This region has been independently found in other strains by our collaborator at The Jackson Laboratory. The overall goal of this project is to identify candidate genes within Chr 17 interval.

We will begin our efforts to identify genetic modifiers by demonstrating that the Chr 17 QTL can alter phenotype in B6 congenic lines carrying the Chr 17 interval derived from SJL (B6.SJL interval specific congenics) and use marker assisted speed congenic techniques to produce B6.chr17-SJL congenics containing the narrowest interval that moves phenotype (Aim 1). As the intervals are narrowed we will use comparative genomics and bioinformatics, including combining the results from experimental crosses with bioinformatics tools and statistical methods, to guide the selection of candidate genes in the interval (Aim 2). We will combine our results with those from our collaborator at The Jackson Laboratory, and perform haplotype block analyses and haplotype association mapping to minimize the number of candidate genes. By identifying a few candidate genes, we will be well positioned to seek extramural funding to probe the candidate genes and SNPs of interest for sequence and tissue specific expression differences between B6 and B6.SJL mice, in order to identify the responsible modifying gene.

Principal Investigator

Terry D. Heiman-Patterson, MD
Professor of Neurology
Drexel University College of Medicine
3021 Arch St., Suite 100
Philadelphia, PA 19104

Other Participating Researchers

Elizabeth Blankenhorn, PhD, Jeffrey S. Deitch, PhD, Guillermo Alexander, PhD - employed by Drexel University College of Medicine

Expected Research Outcomes and Benefits

We anticipate that over the funding year we will be able to complete 7 generations of matings to narrow the interval since we are already at our third generation of matings. Information from these intervals will be used to begin the second step using bioinformatics to narrow the interval and identify candidate gene in the region. We hope to significantly narrow the region of interest and identify several candidate genes over the year of funding. We expect that once we have our initial characterization of the interval specific congenics we will initiate applications for outside funding. The chances of funding will be further enhanced by the actual identification of candidate genes in the region.

Once identified, these candidate genes will help us gain insight into pathways that influence motor neuron degeneration in ALS and provide treatment targets for an otherwise incurable illness.

Summary of Research Completed

Previously we have created genetically homogeneous inbred (congenic) lines of mice that carry the G93A Tg on homogeneous backgrounds and demonstrate differences in survival . Expression of G93A Tg in congenic lines with ALR, NOD.Rag1KO, SJL or C3H backgrounds (SJL.Tg+ and C3H.Tg+) show a more severe phenotype than in the mixed (B6xSJL) background, whereas a milder phenotype is observed in B6, B10, BALB/c and DBA inbred mice. These differences are likely due to a genetic modifier and we have identified a region of chromosome 17 (5.47-35.5 cM) that was significantly linked to survival of TG+ mice in the F2 crosses of SJLXB6 and ALRX B6. The goal of this research project is to identify the candidate genes within Chr 17 interval. During the first 6 months of funding the following progress has been made on the two Aims directed at identifying these candidate genes:

Aim 1: Narrowing the chromosomal 17 interval. The first step is to breed B6 congenic mice carrying both the mutant G93A SOD1 Tg and the Chr 17 intervals from the SJL genetic background. These interval specific congenic mice will be mated to B6 Tg (G93A) mice to obtain the smallest segment of the Chr17 QTL that retains the ability to move phenotype (survival).

We have identified SNPs that differ between SJL and B6 in our Chromosome 17 interval and have defined the SJL interval in our B10.SJL animals. Our B10 animals carry an SJL interval that extends from 32 cM-40cM on Chromosome 17. This interval contains the distal end of the interval of interest. Therefore, if it moves phenotype we will narrow our genes of interest to 4 while if it does not move phenotype, we will reduce the number of genes to 29 (see Table 1 below for the 33 genes we have identified).

We have begun the breeding strategy to obtain mice that are B6.SJL Tg+. First our B10.SJL animals were bred to B6 TG+ G93A mutant mice to create a line in which all the animals were heterozygous for the SJL insert with a mixed B10,-B6 background. The Tg+males from this cross have been back crossed to female nonmutants that are heterozygous and the offspring selected for homozygosity of the SJL insert. Tg+ SJL homozygous males are again chosen and mated to B6 animals. Once again, the resultant offspring are heterozygous at SJL and at N2 for the B6 background. We are about to start breeding for the homozygousity at SJL interval between siblings for N3 and will begin phenotype analysis at the N4.

Aim 2. To identify candidate gene(s) within the narrowed QTL by applying the bioinformatics approach. Over the last 6 months we have narrowed the interval of interest to 2Mb. This was done through our collaboration with Dr. Cox at Jackson Laboratories. This was done through selection of haplotype blocks and the resequencing of the Chromosome 17 intervals of interest to identify nonsynonymous SNPs.

In order to focus only on those areas of the Chromosome 17 QTL which were consistent with our strain lifespan pattern, we utilized the Mouse Strain Comparison web application (http://cgd.jax.org/straincomparison/) at the Center For Genome Dynamics (http://cgd.jax.org/index.shtml) for haplotype analysis. Briefly, long-lived (B6, BALB, DBA) strains were compared to short-lived (ALR, NOD, SJL) strains, using methods suggested on the web application, and requesting a block size of 1000 contiguous SNPs on Chromosome 17. We focused our further efforts only to those regions with SNP haplotypes consistent with short vs long life to design the capture arrays for resequencing.

As the ALR/LtJ and SJL/J strains have not been included in the Sanger mouse resequencing project, we sought to identify potentially functional polymorphisms that were conserved with NOD/LtJ and that differed from the B6, BALB and DBA strains. Five large regions of conserved haplotype blocks based on both genotyped and imputed SNPs in the B6, BALB and DBA strains that differed from the short-lived ALR, NOD and SJL strains were selected to design capture arrays for resequencing the ALR and SJL strains. The regions captured were: Chr17:3257597-3777149; 4044578- 4177855; 10399256- 16152415; 29743643- 37251471 and 43675762-45391511. A custom Agilent 244K probe exome capture array (60 nt probes, with a 5 nt offset) was designed to capture all annotated mouse exons and 5' promoter regions from the ~15.6 Mb identified from the haplotype analysis. A total of 3646 exons and conserved elements were identified for capture and encompassed approximately 1.9 Mb of mouse Chr 17 sequence. The resequenced regions for ALR/LtJ and SJL/J were compared to the sequences from the Wellcome Trust Sanger Institute (http://www.sanger.ac.uk/) for C57BL/6J, NOD/LtJ, C57BL/6J, DBA/2J and BALB/cByJ. Thirty-three genes (see Table 1 below) were identified with non-synonymous SNPs or indels matching the life-span haplotypes.

Table 1

Gene #	Gene Symbol	# of potential coding changes	Gene #	Gene Symbol	# of potential coding changes
1	Tiam2	9	18	Kank3	1
2	Tfb1m	1	19	Psmb8	1
3	Park2	1	20	H2-Eb1	1
4	Igf2r	2	21	H2-Eb2	1
5	Airn	4	22	Egfl8	1
6	Wtap	1	23	C4a	2
7	Sod2	1	24	Stk19	1
8	Gm7168	1	25	C2	1
9	Dact2	4	26	Ehmt2	1
10	Smoc2	1	27	Neu1	4
11	Btbd9	1	28	H2-T23	1
12	RP23-451J17.2	4	29	CT030728.6	1
13	Notch3	2	30	Gm8909	2
14	Ephx3	1	31	AC120403.1	10
15	Wiz	2	32	H2-M10.5	5
16	Cyp4f13	2	33	Olfr90	4
17	4921501E09Rik	1	34	AC116130.1	5

Research Project 6: Project Title and Purpose

Collaborative Analysis of Nuclear Pores: Protein Trafficking and Recognition - This project will increase our understanding of the mechanisms by which the nuclear pore complex (NPC) operates. The NPC is an elaborate cellular machine that controls traffic of macromolecules between the nucleus and cytoplasm of living cells, and as such is critical for normal cellular functions. The NPC plays key roles in the delivery of viral DNA and gene therapy reagents, and its functions are thought to be hijacked or reprogrammed in disease states such as cancer; hence, it is a prime drug target. In addition to producing fundamental biological information about NPC functioning, this project will also produce new tools that will allow for rapid screening of potential drugs that can modulate NPC activity.

Anticipated Duration of Project

1/1/2011 - 12/31/2012

Project Overview

We wish to identify the molecular basis of selective and facilitated transport through the nuclear pore. We propose to do this by using specific protein components drawn from the nuclear pore complex (NPC) to construct both two- and three dimensional models of the nuclear pore. The two-dimensional model renders experimentally accessible the details of processes that take place

inside the depths of a three-dimensional pore; the three-dimensional model allows for the validation of findings made on the two-dimensional model. This approach can be expected to result in unambiguous conclusions about the mechanisms of transport.

The two-dimensional model will consist of selected FG-repeat proteins, immobilized on the surface of a quartz crystal microbalance at densities appropriate for brush formation. Use of the microbalance will allow us to directly measure changes in brush height and conformation. The three-dimensional model will be constructed using nanopore membranes of aluminum oxide; these membranes contain dense arrays of pores having highly monodisperse diameters (e.g., 20 nm, 35 nm, 50 nm) that coincide with published estimates of the central channel diameter in the NPC. FG-repeat proteins will be grafted within these pores, and the ability of the pores to facilitate trafficking will be assessed by passing solutions through the membranes that contain various proteins, including molecules of different sizes that contain no nuclear import or export sequences (to probe the size cut-off) and cargo molecules with the appropriate import/export sequences, in the presence or absence of transportins (to test for transportin-mediated selective trafficking). Such model systems offer complete control over experimental parameters, allowing us to test with great precision the exact contribution of different constituents of the system (for example, by using site-directed mutants of different FG-repeat proteins).

Principal Investigator

Patrick J. Loll, PhD
Professor
Drexel University College of Medicine
Department of Biochemistry and Molecular Biology
245 N. 15th St.; MS 497
Philadelphia, PA 19102

Other Participating Researchers

Lynn S. Penn, PhD - employed by Drexel University

Expected Research Outcomes and Benefits

At a fundamental level, the proposed work will generate new insights into the functioning of the nuclear pore complex (NPC), one of the most intricate and important macromolecular machines to be found in living cells. At a practical level, the proposed work will lead to the production of a novel NPC model—a simple semi-synthetic system that mimics the transport behavior of authentic NPCs. Unlike actual NPCs, which can only be obtained in minute quantities by laborious purification from biological materials, the model pores will be readily scaled up, and should prove very useful in high-throughput screens to identify agents that can modulate the trafficking of specific target molecules. This contributes to improved public health by streamlining the discovery of new therapeutic agents.

Summary of Research Completed

Because funding did not become available until well into the project period, and because of the delays associated with recruiting a suitable research assistant to perform the projected research, this project has only recently begun to progress at full speed. Note that this is not a surprise; both sources of delay were anticipated and incorporated into our planning process, and are reflected in the projected end date of the project. Having said this, we have so far made progress in several areas.

First, we have identified a research assistant, Laura Alexander, who joined the project at the beginning of June and will be primarily responsible for its implementation. Ms. Alexander was recruited after a careful search that involved solicitation of applications from Departments of Chemistry at highly ranked four-year colleges in the Philadelphia area. We received applications from many outstanding candidates; Ms. Alexander was our first choice, and we are gratified that she has accepted the position. She is an alumna of Bryn Mawr College with extensive research experience in chemistry.

Ms. Alexander has begun the molecular biology required to prepare expression constructs for the production of our target FG-repeat proteins. She has successfully amplified genes for our two protein targets (Nsp1 and Nup145) from *S. cerevesiae,* and is currently subcloning these genes into an in-house expression vector. Preliminary results suggest that one of these subcloning experiments has already succeeded, and we anticipate that the other will follow closely. This is excellent progress for the relatively brief period of time during which Ms. Alexander has been associated with the project.

On another front, Dr. Chengjun Sun, a postdoctoral researcher in Dr. Penn's laboratory, has made good progress in developing the techniques that will allow us to specifically immobilize our FG-repeat proteins on solid surfaces, such as the sensor of the quartz crystal microbalance and the walls of model pores. Specifically, he has developed chemistry that allows him to couple cysteine residues via their carboxyl groups to polymers that, in turn, are themselves immobilized on a quartz surface; he was then able to remove protecting groups from the amino acid's amino group and side chain, leaving a native cysteine residue appropriate for our projected native chemical ligation strategy. This work has been assembled into a manuscript and has been submitted.

Research Project 7: Project Title and Purpose

Can Up-regulation of Glutamate Transporters Be Protective in Traumatic Brain Injury? - The purpose of this project is to investigate if a glutamate transport activator, Parawixin1, has protective effects on the pathology of traumatic brain injury (TBI). This hypothesis is suitable since TBI increases extracellular levels of glutamate resulting in injured tissue, membrane depolarization and calcium influx that activates phospholipases, endonucleases and proteases that can lead to apoptosis. Rats will be subjected to moderate TBI and glutamate transport with radioactive assays will be performed in synaptosome preparations of the brains of rats injected with Parawixin1 prior and after the injury. In addition, analyses of edema, tissue loss, activation of calpain and loss of neuronal MAP-2 (markers of neurodegeneration and apoptosis) will be

done. This knowledge could provide new therapeutical strategies for amelioration of the secondary outcomes of TBI.

Anticipated Duration of Project

1/1/2011 - 12/31/2012

Project Overview

The project research objective is to investigate the effects of a glutamate transport activator, Parawixin1, on different aspects of the pathology of traumatic brain injury (TBI). The specific Aims are:

1. To investigate the effects of Parawixin1 on glutamate uptake in rat brain synaptosomes isolated from rats subjected to TBI. In this aim we will determine whether administration of Parawixin1 to rats either prior to or following TBI will stimulate glutamate transport in rat brain synaptosomes. Two groups of animals will be designed; the first one will receive intravenous injections of either saline or two doses of Parawixin1 before the injury and the second group will receive the injections after the injury. Lateral fluid-percussion brain injury will be performed. Cortex and hippocampus from both groups will be dissected, frozen and synaptosomes will be prepared. A pre-incubation with Parawixin1 or vehicle in 96 wells plates will be followed by the addition of ^{3}H-L-glutamate to synaptosomes. To finish uptake reactions plates will be filtered, washed and radioactivity will be measured. ED_{50} will be calculated for the effects of Parawixin1 as well kinetic analyses of glutamate transport.

2. To investigate effects of Parawixin1 on regional brain edema following TBI in the rat. Two groups of animals will be designed; the first one will receive either saline or two doses of Parawixin1 at the completion of surgery and injury will be performed 15 min later. The second one will receive the injections after the injury. Brains from both experimental groups will be dissected into cortex and hippocampus and analyzed for water content using the wet weight/dry weight method, as increase in tissue water content is an indication of edema.

3. To investigate effects of Parawixin1 on acute calpain and caspase-3 activation, loss of neuronal MAP-2, blood-brain barrier breakdown and neurodegeneration following TBI in the rat. Two groups of animals will be designed; the first one will receive either saline or two doses of Parawixin1 after surgery and injury will be performed 15 min later. The second group will receive Parawixin1 administration following injury. At 24 hours, animals from each treatment group will be anesthetized, transcardially perfused with heparinized saline followed by 10% formalin, and brains processed for histologic evaluation. Stainings with cresyl violet (Nissl), fluoroJade B and for calpain activation to detect extravasation of blood-borne IgG via a breakdown of the blood-brain barrier will be done. Immunoreactivity will be quantified by outlining the area of Ab38- or IgG-stained tissue in the injured quadrant. Loss of MAP-2 immunoreactivity will be quantified by outlining the area of absent staining.

Principal Investigator

Andréia C. K. Mortensen, PhD
Research Assistant Professor
Drexel University College of Medicine
245 North 15th Street, MS 488
Room 10315 NCB
Philadelphia, PA 19102

Other Participating Researchers

Ramesh Raghupathi, PhD - employed by Drexel University College of Medicine

Expected Research Outcomes and Benefits

The expected outcomes and benefits of this research project are:

1) We anticipate that Parawixin1 will augment glutamate transport from rats subjected to TBI. We will test whether injection of Parawixin1 prior or subsequent to TBI will have an effect on glutamate transport and will reduce excitotoxic damage in the traumatically-injured rat brain.

2) We also expect to observe a dose-dependent decrease in fluoro-jade B(+) cells in the cortex and hippocampus, although we are not sure whether this result would appear from pre-injections or post-injection of Parawixin1. In part, traumatic neurodegeneration may be mediated by calpain activation, which, in turn may be activated by ionotropic glutamate receptors. Reducing the concentration of extracellular glutamate may therefore be associated with less calpain activation and fewer apoptotic cells.

3) Similarly, based on observations that both ionotropic receptor antagonists and glutamate release blockers reduce edema, we expect that pre or post-injection of Parawixin1 will reduce edema in the cortex and hippocampus at 24h post-injury.

4) Therefore this funding will help establishing a new research group that can likely generate interdisciplinary research data to compete for an application for extramural support on neuroscience research.

5) This kind of investigation has never been done before; the levels of glutamate after TBI in synaptosomal preparations of the brains are unknown, and also unknown are the potential effect of direct glutamate transport activators on these levels and other secondary measurements. This knowledge could establish potential therapeutical routes and windows for treatment of secondary injuries of TBI.

Summary of Research Completed

For Aim number 1 a fundamental piece of equipment, a *Unifilter-96 Cell Harvester from Perkin Elmer* was purchased and installed. We have begun to set up the experiments which included

performing the traumatic brain injuries to the rats injected with Parawixin1, isolating brain tissues and performing glutamate uptake assays in synaptosomes. We are now optimizing our uptake protocols in synaptosomes.

Research Project 8: Project Title and Purpose

Mechanisms of Carbon Monoxide Mediated Hypercoagulability - Exposure to tobacco smoke has been associated with a variety of chronic and acute diseases, one of which is thrombotic disease (e.g., acute coronary syndrome, stroke). Among the many constituents of smoke, carbon monoxide (CO) has long been recognized as an important poisonous component. Critically, it has been recently recognized that exposure of human plasma to CO concentrations well within the range encountered during smoking results in enhanced coagulation and diminished fibrinolysis *in vitro*. The purpose of this project to further define the molecular mechanisms by which this occurs, specifically focusing on the heme-mediated modulation of fibrinogen and α_2-antiplasmin function by CO. It is anticipated that these insights will significantly impact on future diagnostic and prognostic management of patients exposed to CO.

Anticipated Duration of Project

1/1/2011 - 12/31/2012

Project Overview

Preliminary manuscripts have demonstrated that fibrinogen, the primary plasmatic substrate of coagulation, and α_2-antiplasmin, the most important antifibrinolytic enzyme, are the proteins modified by CO. Further, CO-mediated modification of fibrinogen as a substrate for thrombin is likely dependent on a heme attached to fibrinogen. These are the first data demonstrating that gas-sensing molecules exist in the coagulation/fibrinolytic pathways. *Thus, our central hypothesis is that CO-mediated modification of fibrinogen and α_2-antiplasmin may play a major role in acquired hypercoagulability.* To test this hypothesis and gain mechanistic insight into these phenomena we plan to complete the following specific aims:

> *1. Define CO and/or heme structural modification of fibrinogen and α_2-antiplasmin.*
> *2. Mechanistically assess CO-induced/heme-based modification of fibrinogen and α_2-antiplasmin mediated hypercoagulability.*

The following brief descriptions of experimentation outline the approaches planned to achieve our goals:
Fibrinogen Studies: We will use conditions (including acetonitrile gradients) to determine release of heme from specific subunits of fibrinogen with intact protein mass spec.
α_2-antiplasmin Studies: Identification of a putative α_2-antiplasmin associated heme and the molecular location of attachment or other CO mediated modifications will be identified by mass spec.
Heme Group Modulation Experiments: Normal plasma and purified fibrinogen/α_2-antiplasmin will be exposed to reductants to render the heme unresponsive to CO, identifying CO mediated hypercoagulation.

CO Catalysis/Scavenging Experiments: Normal plasma and purified fibrinogen/α_2-antiplasmin will be exposed to reductants to render the heme unresponsive to CO, identifying CO mediated hypofibrinolysis.

Principal Investigator

Vance G. Nielsen, MD
Professor
Drexel University College of Medicine
Department of Anesthesiology
Mail Stop 310
Broad & Vine Streets
Philadelphia, PA 19102

Other Participating Researchers

Keith Vosseller, PhD, Matthew Nowak - employed by Drexel University College of Medicine

Expected Research Outcomes and Benefits

Our research will establish a molecular biology-based method to target modifications within the coagulation/fibrinolytic system and subsequently test the physical chemical relevancy of these modifications in a plasma-based hemostasis assessment system that is clinically relevant. The ability to identify and perhaps stratify populations at risk of thrombosis secondary to CO exposure will likely be realized. Further, being the investigators that made the original observations that the coagulation/fibrinolytic systems contain gas-sensing molecules will set the stage for future granting/collaborative efforts in both basic and clinical areas. It is anticipated that the diagnostic tool designed and validated by this project will qualify as an invention and will likely require collaboration with extramural funding sources to clinically test and license.

Summary of Research Completed

In order to achieve the aforementioned specific aims, we have initially pursued two different lines of investigation that are outlined subsequently by project.

Heme Group Modulation Experiments: Normal plasma and purified fibrinogen/α_2-antiplasmin will be exposed to reductants to render the heme unresponsive to CO, identifying CO mediated hypercoagulation.

Based on our previous work, we used a redox-based approach to render fibrinogen-bound heme unresponsive to addition of CO and subsequently extended this method to outcompete/remove CO bound to fibrinogen associated heme.

Pooled normal plasma (George King Bio-Medical, Overland Park, KS, USA) anticoagulated with sodium citrate was utilized for experimentation. The final volume for all subsequently described plasma sample mixtures was 359.2 µl. Sample composition consisted of 322 µl of

plasma; 10 µl of tissue factor reagent (0.1% final concentration in dH_2O; Instrumentation Laboratory, Lexington, MA, USA), 3.6 µl of dH_2O or dH_2O containing the organic reductant phenylhydroxylamine (PHA, 0-30 mM final concentration, Sigma-Aldrich, Saint Louis, MO, USA), 3.6 µl of dimethyl sulfoxide (DMSO) or DMSO with CORM-2 (0-400 µM final concentration; Sigma-Aldrich) and 20 µl of 200 mM $CaCl_2$. PHA was chosen as the agent to convert fibrinogen-associated, heme-bound Fe^{+2} to an Fe^{+3} state as PHA is the most rapid and efficient metheme forming agent. Such an agent would be required, given the marked avidity of CO for heme groups with Fe^{+2} states present. Stock solutions of CORM-2 were made just before each experiment. Tissue factor stock solution was kept on ice prior to use and was remade every two hours. Plasma sample mixtures were placed in a disposable cup in a computer-controlled thrombelastograph® hemostasis system (Model 5000, Haemoscope Corp., Niles, IL, USA), with addition of $CaCl_2$ as the last step to initiate clotting. Data were collected for 15 min at 37°C. Given that final clot strength is the *sine quo non* of fibrinogen concentration in plasma, and that elastic modulus (G, dyne/cm^2) is a measure of strength that can be determined by all commercially available thrombelastographs/thromboelastometers, G values were subsequently recorded for all samples. Lastly, all conditions were represented by n=6-8 replicates per condition.

We successfully prevented CO-mediated enhancement of plasma clot strength using a thrombelastograph to assess coagulation kinetics as indicated in figure 1. The first column (No C, No P) indicates the results of strength (G) of plasma not exposed to either 10 mM PHA (P) or 100 µM CORM-2 (C). Addition of CORM-2 significantly increased G compared to unexposed plasma (*$P<0.05$), and addition of PHA alone (No C, P) significantly decreased G compared to unexposed plasma or CORM-2 exposed plasma (†$P<0.05$). Lastly, plasma exposed to PHA before CORM-2 (P,C) displayed G values slightly different from unexposed plasma, but also clearly different from CORM-2 exposed plasma and PHA exposed plasma (‡$P<0.05$).

Using the same paradigm, but instead exposing plasma to CO prior to PHA exposure, we determined that addition of 30 mM PHA was required to attenuate the CO-mediated enhancement of clot strength. These data are displayed in figure 2. Additional experiments demonstrated that pretreatment of plasma with 30 mM PHA could not be overcome with up to 400 µM CORM-2, and these results are displayed in figure 3. These and other supporting data were accepted in manuscript form at the journal *Blood Coagulation & Fibrinolysis*, and the described assay of carboxyhemefibrinogen-mediated hypercoagulability has been submitted to Drexel University's Office of Technology Commercialization. Filing for protection of intellectual property and patent are being performed and will be completed by the first week of July.

<u>α_2-antiplasmin Studies: Identification of a putative α_2-antiplasmin associated heme and the molecular location of attachment or other CO mediated modifications will be identified by mass spectrometry.</u>

Following the preceding experimentation, we attempted to use the same approach with PHA to detect CO mediated hypofibrinolysis in human plasma as documented with thrombelastography, with a notion that this hypofibrinolytic state was mediated by CO-mediated enhancement of α_2-antiplasmin. The methodology used was similar, with the addition of tissue-type plasminogen

activator (tPA) to lyse the formed thrombus. However, we instead found that exposure of plasma to metheme forming agents (PHA and a nitric oxide donor, MAHAMA-NONOate) instead induced a hypofibrinolytic state in the absence of CO as displayed in tables 1 and 2. In order to determine if α_2-antiplasmin activity was enhanced by either a carboxy or met hemoglobin state, purified α_2-antiplasmin was exposed to either CORM-2 or MAHMA-NONOate and then placed in α_2-antiplasmin-deficient plasma. As seen in figure 4, NO enhanced lysis (decreased α_2-antiplasmin activity) whereas CO attenuated lysis (increased α_2-antiplasmin activity). This result indicated that a potential decrease in plasmin activity was responsible to the antifibrinolytic effect observed by conditions favoring metheme states. Purified plasmin was exposed to MAHMA-NONOate or CORM-2 and then placed into normal plasma where increases in plasmin activity equate to a reduction of the velocity of clot growth and strength. As demonstrated in figure 5, pretreatment of plasmin with MAHMA-NONOate decreased its activity – very similar results were obtained following CORM-2 exposure.

We attempted to identify heme attached to α_2-antiplasmin with mass spec, but have been unsuccessful secondary to glycosylation of the enzyme, which impedes proteolysis. We are utilizing an approach to digest the attached sugars at present and anticipate positive results. Mass spec analysis of plasmin readily demonstrated the presence of a heme groups as displayed in figure 6. This second line of investigation is under review in manuscript form at *Blood Coagulation & Fibrinolysis*.

In sum, we have successfully created an assay to detect carboxyhemefibrinogen-mediated hypercoagulation and are seeking a patent of same. We have also discovered another, unexpected heme modulation of a key enzyme in the fibrinolytic pathway. Given that simultaneous modulation of the putative heme attached to α_2-antiplasmin and the heme attached to plasmin summates as hypofibrinolysis, a redox-based method to assess CO-mediated hypofibrinolysis cannot be established. Thus, creation of a CO-catalyzing assay will be required to assess CO-mediated hypofibrinolysis.

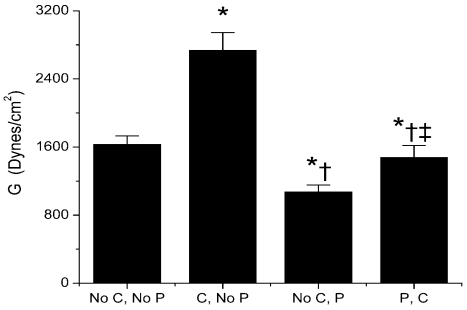

Figure 1. Experiments to prevent CO binding to fibrinogen-bound heme. Data presented as mean+SD. C = 100 μM CORM-2, P = 10 mM PHA, no C = 0 μM CORM-2, no P = 0 mM PHA. *P<0.05 vs. No C, No P; †P<0.05 vs. C, No P; ‡P<0.05 vs. No C, P

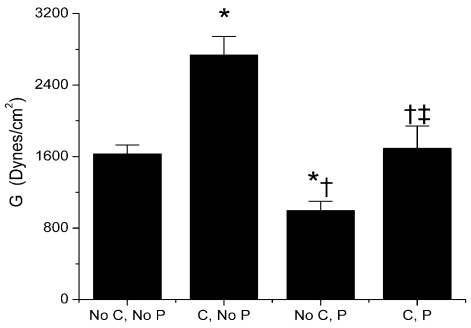

Figure 2. Experiments to remove CO from fibrinogen-bound heme. Data presented as mean+SD. C = 100 μM CORM-2, P = 30 mM PHA, no C = 0 μM CORM-2, no P = 0 mM PHA. *P<0.05 vs. No C, No P; †P<0.05 vs. C, No P; ‡P<0.05 vs. No C, P.

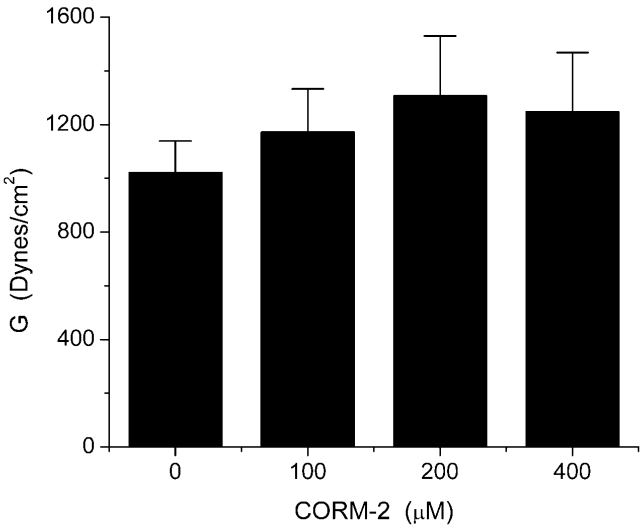

Figure 3. Experiments to determine irreversibility of PHA-mediated oxidation of fibrinogen-bound heme with addition of CO excess. Pretreatment with 30 mM PHA prevented CORM-2 mediated increases in G values.

Table 1. Effects of PHA on tPA mediated fibrinolysis in normal, pooled plasma.

Condition	0 mM	5 mM	10 mM
TMRTG	3.0(2.2,3.2)	2.9(2.9,3.0)	3.6(3.5,3.8)*†
MRTG	5.0(4.4,6.5)	4.2(4.0,4.7)	3.5(3.2,3.8)*†
TTG	113(101,119)	96(90,102)	89(80,96)*†
TMRL	7.5(5.0,9.4)	6.9(6.1,11.3)	9.7(6.6,11.4)
MRL	-0.9(-1.1,-0.8)	-0.7(-0.9,-0.6)*	-0.7(-0.8,-0.7)*
CGT	3.0(2.6,3.6)	3.8(2.9,4.2)	5.0(4.2,5.2)*†
CLT	14.6(12.5,15.0)	16.7(12.5,20.9)	17.9(14.2,18.4)
CLS	17.4(15.4,18.9)	20.0(15.8,25.0)	21.8(19.4,23.6)

Data are presented as median (1^{st}-3^{rd} quartiles). TMRTG = time to maximum rate of thrombus generation (min); MRTG = maximum rate of thrombus generation (dynes/cm^2/sec); TTG = total thrombus generation (dynes/cm^2); TMRL = time to maximum rate of lysis (sec); MRL = maximum rate of lysis (-dynes/cm^2/sec); CGT = clot growth time (min); CLT = clot lysis time (min); CLS = clot lifespan (min). *P<0.05 vs. 0 mM PHA, †P<0.05 vs. 5 mM PHA.

Table 2. Effects of MAHMA NONOate on tPA mediated fibrinolysis in normal, pooled plasma.

Condition	0 mM	1 mM	2 mM
TMRTG	2.5(2.5,2.6)	3.1(3.0,3.2)*	2.7(2.5,2.7)*†
MRTG	5.8(5.2,6.3)	4.4(4.1,4.8)*	6.0(5.6,6.5)†
TTG	120(107,127)	94(86,101)*	118(109,131)†
TMRL	7.9(6.6,9.4)	6.2(4.3,6.9)*	13.4(9.2,15.0)*†
MRL	-1.1(-1.2,-1.0)	-1.2(-1.3,-1.0)	-1.2(-1.3,-1.0)
CGT	3.1(2.6,3.4)	2.7(2.6,2.9)	3.8(3.2,4.5)*†
CLT	13.0(12.6,13.6)	11.3(9.7,13.4)	18.2(16.0,23.0)*†
CLS	16.2(15.56,17.0)	14.2(12.1,16.2)	22.6(19.1,26.6)*†

Data are presented as median (1^{st}-3^{rd} quartiles). TMRTG = time to maximum rate of thrombus generation (min); MRTG = maximum rate of thrombus generation (dynes/cm^2/sec); TTG = total thrombus generation (dynes/cm^2); TMRL = time to maximum rate of lysis (sec); MRL = maximum rate of lysis (-dynes/cm^2/sec); CGT = clot growth time (min); CLT = clot lysis time (min); CLS = clot lifespan (min). *P<0.05 vs. 0 mM PHA, †P<0.05 vs. 1 mM MAHMA NONOate.

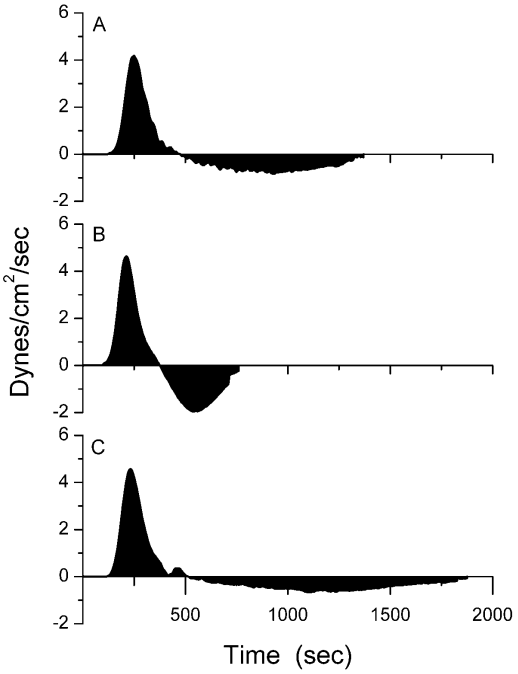

Figure 4. Effects of NO and CO on isolated, purified α_2-antiplasmin activity. Panel A: Fifty μg/ml of α_2-antiplasmin was added to α_2-antiplasmin deficient plasma in the presence of tPA. Panel B: NO derived from MAHMA NONOate was added to α_2-antiplasmin prior to reaction, accelerating fibrinolysis. Panel C: CO derived from CORM-2 was added to α_2-antiplasmin prior to reaction, attenuating fibrinolysis.

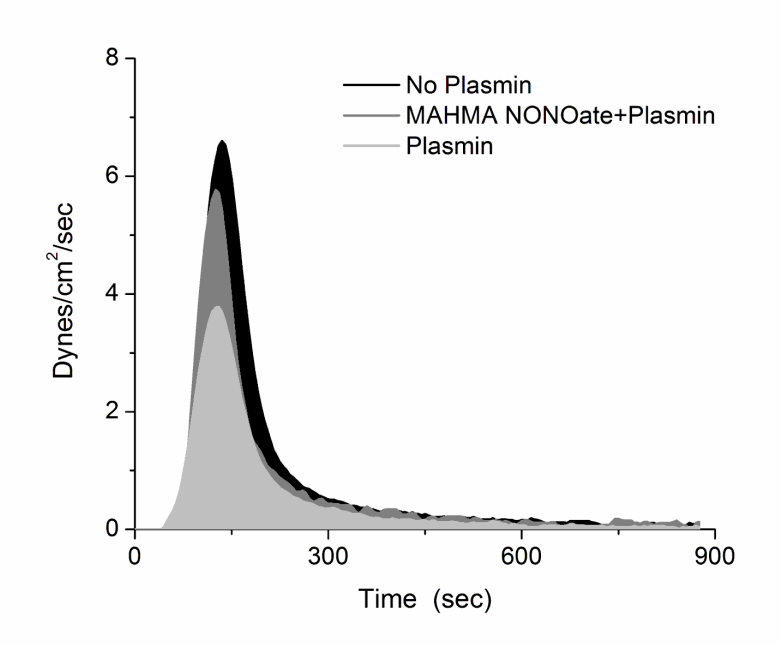

Figure 5. Effects of NO on isolated, purified plasmin activity. Coagulation in normal plasma (black trace) was inhibited by addition of plasmin (light gray trace). Plasmin exposed to NO derived from MAHMA NONOate (gray trace) decreased coagulation to a significantly lesser extent than unexposed plasmin.

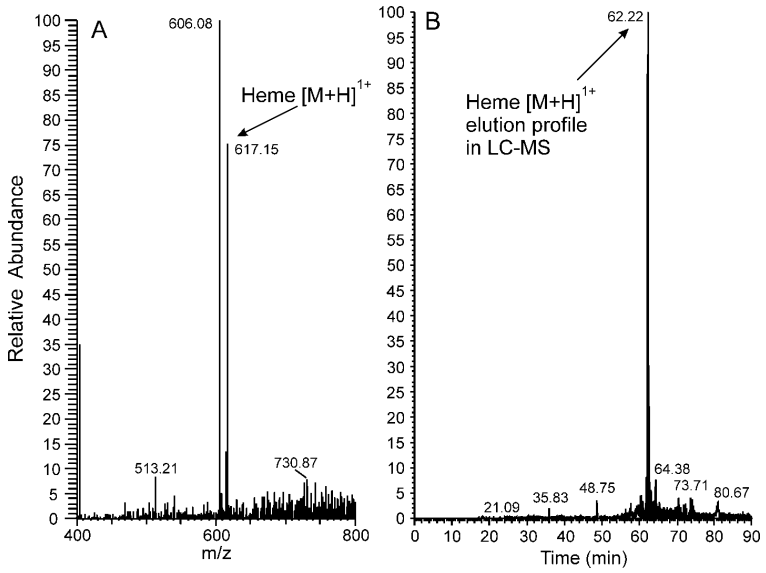

Figure 6. Evidence of free heme in tryptic digest of human Plasmin. Panel A: A reverse phase LC-MS/MS analysis of a tryptic digest of human purified plasmin; the full MS scan reveals a m/z 617.15, corresponding to singly charged reduced heme. Panel B: An extracted ion chromatogram of m/z 617.15 reveals the heme elution time of 62.22 minutes during LC-MS/MS.

Research Project 9: Project Title and Purpose

Role of Cytoskeletal Dynamics in Radiation-Induced Breast Cancer Invasion - The goal of the proposed research is to investigate the role of cytoskeletal-associated pathways in regulating radiation-induced invasion in ErbB2-positive breast cancers. We hypothesize that changes in cytoskeletal pathways that regulate neuronal branching may play a significant role in breast cancer cell invasion and invadopodia formation, and may offer novel therapeutic targets for treating invasive breast cancer including radiation-induced progression of pre-malignant state to invasive breast cancer. I propose to unveil new aspects of cancer invasion and to test relevant potential therapeutic targets for blocking the invasion of breast cancer cells using 3D cell culture systems developing in my laboratory.

Anticipated Duration of Project

1/1/2011 - 12/31/2012

Project Overview

Metastatic dissemination is responsible for the majority of treatment failures and death of patients with breast cancer. Understanding the mechanism whereby breast cancer cells execute invasive and metastatic spread may provide the foundation necessary for treatment of the disease. Approximately 25% of breast cancer diagnoses are of the “premalignant” non-invasive condition ductal carcinoma *in situ* (DCIS). DCIS carries a similar therapeutic regimen to its

invasive counterpart, including radiation therapy. Although most patients who receive local therapy for DCIS do not progress to invasive/metastatic disease, concern regarding the necessity of radiation therapy in DCIS treatment is growing. Inclusion of radiotherapy reduces local recurrence, but it has *no statistically significant survival benefit* and been shown to promote a *higher rate of contralateral breast cancer.* ErbB2 overexpression is associated with pro-metastatic pathways and resistance to radiation therapy. Radioresistance alters cellular interactions with the microenvironment, which could play a role in invasion, contraindicating radiation therapy for ErbB2-expressing tumors. To simulate tissue-specific cellular interactions that may underlie physiologically relevant responses to ionizing radiation (IR), we cultured with exogenous extracellular matrix (Matrigel) nontransformed human MCF10A mammary epithelial cells overexpressing ErbB2 oncogene (MCF10A-ErbB2) to generate three dimensional (3D) non-invasive, filled structures characteristic of DCIS. We have shown, for the first time, that MCF10A-ErbB2 mammary structures exposed to high energy (6MV) X-rays at a dose of 2Gy showed invasive projections into Matrigel beginning 4 days post-treatment. To invade new tissues, breast cancer cells degrade the ECM through release of matrix metalloproteinases (MMPs) from finger-like projections, called invadopodia. Invadopodia are actin-based protrusive structures and the invasion of microtubules into invadopodia is required for their stabilization and function. *There are notable similarities between invadopodia and the formation of new branches from the axons of developing neurons*. In this CURE application, *we hypothesize that changes in cytoskeletal pathways that regulate neuronal branching may play a significant role in breast cancer cell invasion and invadopodia formation, and may offer novel therapeutic targets for treating invasive breast cancer including radiation-induced progression of pre-malignant state to invasive breast cancer.*

Principal Investigator

Mauricio J. Reginato, PhD
Assistant Professor
Drexel University College of Medicine
Department of Biochemistry & Molecular Biology
245 N. 15th Street, MS497
Philadelphia, PA 19102-1192

Other Participating Researchers

Peter Baas, PhD, Gianluca Gallo, PhD, Diane Kambach, Lee Silver, Wenqian Yu – employed by Drexel University College of Medicine

Expected Research Outcomes and Benefits

The hypothesis underlying the proposed work is extremely innovative in current breast cancer research. The hypothesis is paradigm shifting and suggests that there is a connection between ionizing radiation (IR) and progression from a premalignant to malignant breast cancer via formation of invadopodia in ErbB2 positive breast cancers. There is great interest in understanding how premalignant breast cancer, such as ductal carcinoma in situ (DCIS) can progress to invasive breast cancer and how to predict risk of progression for each patient. The

potential of ionizing radiation (IR), which is used to treat DCIS, to promote progression to invasive cancer has to our knowledge not been considered. Demonstration that IR treatment of DCIS models in vitro (and in future animal models) results in development of traits of invasive breast cancer and identification of cytoskeletal pathways involved would create a field of study concerning novel markers and potential targets for therapeutic intervention in breast cancer. Our work will yield important novel information on the potential contribution of IR to cytoskeletal signaling, as well as provide an intellectual basis for other researchers in the field of breast cancer signaling to examine relationships between neuron axonal branching and cancer invasion in their own systems related to understanding mechanisms of oncogenic progression and signaling.

Summary of Research Completed

Aim 1: Elucidate the role of phosphoinositide 3-kinase (PI3K) and the Arp2/3 actin nucleation complex in the formation of invadopodia and cancer cell invasiveness.
During this reporting period we have continued to characterize the effect of radiation on ErbB2-positive breast cancer cells. We now show that ErbB2 overexpressing breast cancer cells BT-474 cells become invasive when treated with 2Gy X-Ray similar to what is seen in MCF-10A cells engineered to overexpress ErbB2 (Figure 1A (top), 1B). In contrast, breast cancer (MCF-7) or parental MCF-10A cells that do not express ErbB2 do not undergo invasion following treatment with radiation (Figure 1A (bottom), 1B). Moreover, radiation, induces activation of ErbB2 kinase activity (Figure 1C) by a yet unknown mechanism.

We have also shown that inhibitor of PI3 kinase (LY) is able to nearly completely block radiation-induced invasion in MCF-10A-ErbB2 expressing cells using invasion chamber slides (Figure 2). Use of MEK inhibitor (UO126) was also able to partially inhibit radiation-induced invasion suggesting that multiple signaling pathways may contribute to invasion (Figure 2). Consistent with this data, we find that treatment of MCF-10A-ErbB2 cells with radiomimetic drug neocarzinostatin, which also induces invasion, increases Akt activity in a time-dependent manner (Figure 3). Moreover, we provide data that suggests that activation of PI3K is sufficient to induce cell invasion as treatment of MCF-10A-ErbB2 cells with cell permeable PI3K-activating peptide (PI3Kpep) induces a two-fold increase in cell invasion compared to control cells (Figure 4). We have also begun to optimize breast cancer cells transfected with GFP-PH to monitor PI3K activity in breast cancer cells invading through extracellular matrix. The white arrow in Figure 5 shows a presumed invadopodia-like structure of the highly invasive MDA-MB-231 cells, essentially a bulbous structure protruding in the z-axis. The green arrow denotes the same structure with the PH-GFP and phase overlaid to show that the presumed invadopodia contains what appears to be an accumulation of PH-GFP. The rest of the GFP signal is from the main cell volume in that focal plane. Since this is widefield, the signal denoted by arrows in the invadopodia-like structure is rather strong compared to the signal in the much larger cellular volume represented by the larger halo of green below the invadopodia. We are currently examining PH-GFP in MCF-10A-ErbB2 cells treated with radiation and/or radiomimetic drugs to characterize PI3K activity in invadopodia. In addition, we have characterized two different types of invasion in MCF-10A-ErbB2 cells treated with radiation. We detect both amoeboid-type invasion as well as invadopodia-type protrusions (Figure 6). We are currently further quatifying this phenotype.

Although understanding PI3K activation and regulation of invadopodia in cancer cell invasion was one of the key aspects of this aim, a recent publication has characterized the role of PI3K in breast cancer invadopodia (J. Cell Biology 2011 Jun 27 193 p1275). Thus we will focus work in the next 6 months on more novel aspects of this aim including the role of localized translation of cortactin and WAVE proteins in IR-mediated invasion. We will also focus on examining effects of Arp2/3 inhibitors on invadopodia formation following treatment with radiation.

Aim 2. Determine the efficacy of microtubule-based strategies in mitigating invadopodial activity of breast cancer cells.

The first evidence that microtubule-severing proteins, namely spastin, is involved in cancer cell migration has been reported by our collaborator Dr. Peter Baas (Microtubule-Severing ATPase Spastin in Glioblastoma Multiforme: Increased Expression in Human Glioblastoma Cell Lines and Inverse Roles in Cell Motility and Proliferation Journal of Neuropathology and Experimental Neurology. *in press*). We will examine the role of spastin, katanin-5 & -12 in radiation-induced invasion in breast cancer cells during the next 6-month period.

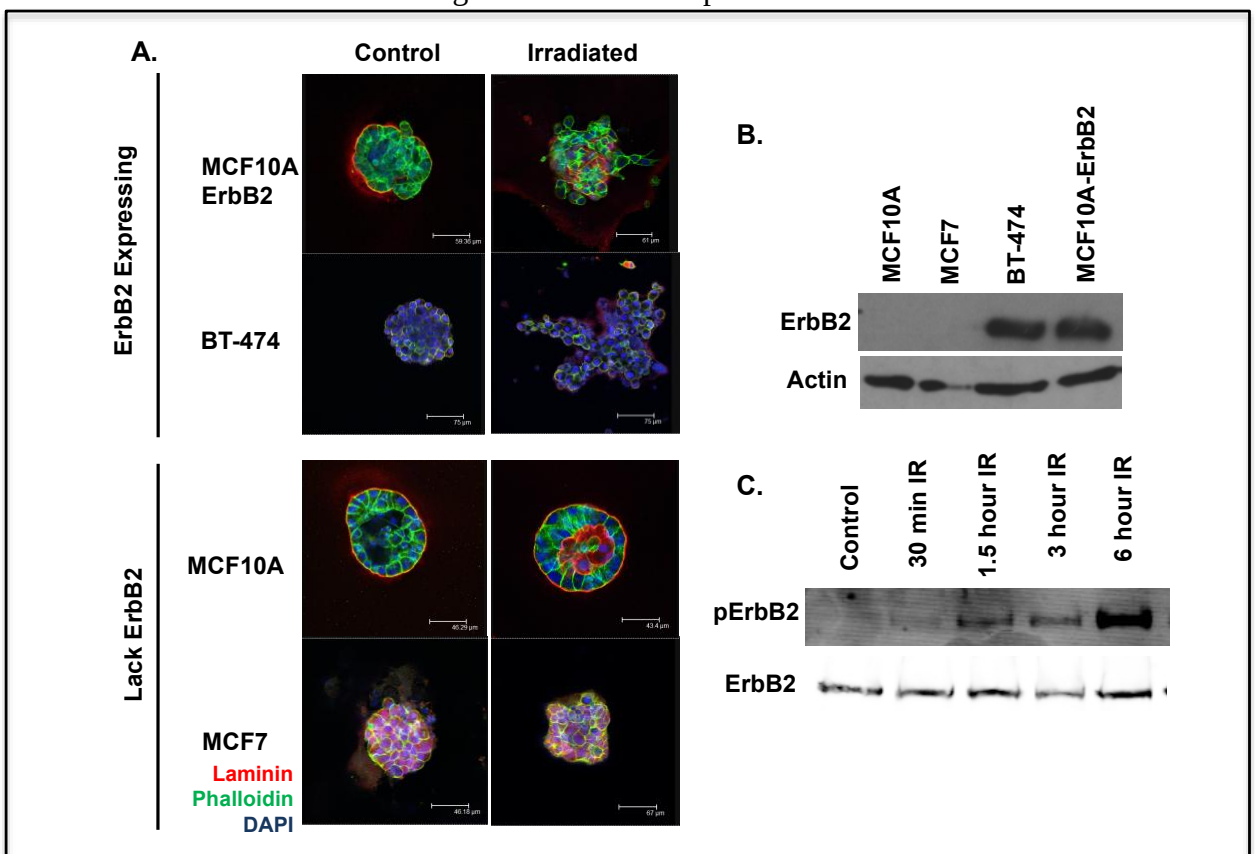

FIGURE 1. Radiation induces invasion in a ErbB2-dependent manner. A. MCF10A- ErbB2 cells and BT-474 cells, which both express ErbB2, become invasive upon treatment with 2 Gy X-rays. MCF10A and MCF7 cells, which lack ErbB2, show no morphological changes upon radiation treatment. Red: laminin; Green: Phalloidin; Blue: DAPI. All images taken 14 days post-irradiation. *B.* Basal ErbB2 expression in four cell lines: MCF10A, a normal mammary epithelial cell line, the breast cancer cell lines MCF 7 and BT-474, and MCF10A cells into which ErbB2 has been transduced. *C.* ErbB2 becomes phosphorylated in MCF10A- ErbB2 cells upon treatment with 2 Gy X-rays.

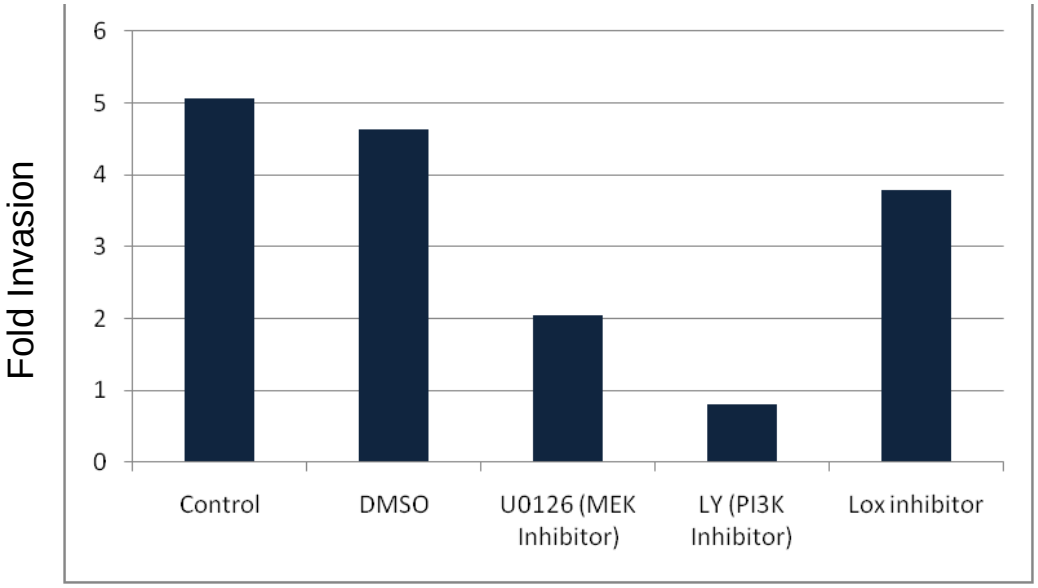

FIGURE 2. Radiation induced invasion is blocked by PI3 Kinase and MEK inhibitor. MCF10A-ErbB2 cells were treated with inhibitor 90 minutes prior to irradiation and analyzed 24 hours after irradiation. MCF10A cells were assayed for ability to invade through Matrigel-coated transwell membranes. Data represented as relative invasion compared to mock radiated cells. Inhibitors used: U0126 (MIK inhibitor, 10μM), LY294002 (PI3 kinase inhibitor, 50μM), Lysyl oxidase (LOX inhibitor, 10μM). Cell viability was checked for all inhibitors to confirm that the cells were not dying.

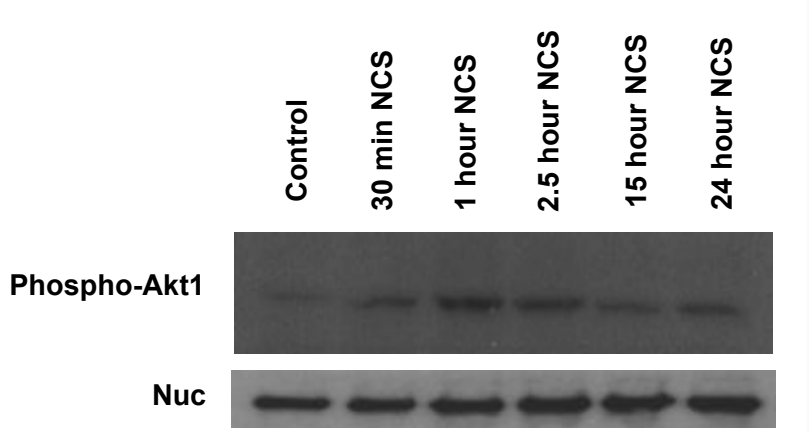

FIGURE 3. Radiomimetics activate AKT. MCF 10A-Erb B2 cells treated with 25ng/ml with the radiomimetic drug Neocarzinostatin (NCS) for indicated times. Cells were lysed and subjected to immunoblotting with the indicated antibodies.

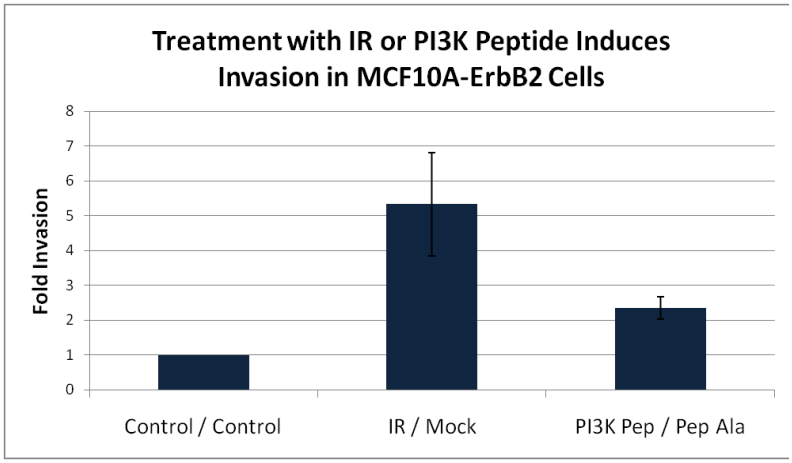

FIGURE 4. Matrigel invasion assays were utilized to determine the effect of 2 Gy ionizing radiation or PI3K-activating peptide on invasion on MCF10A-ErbB2 cells. Mock irradiated cells were treated identically to irradiated cells without receiving IR treatment. Pep-Ala cells were treated with an inactive peptide similar to PI3K-pep.

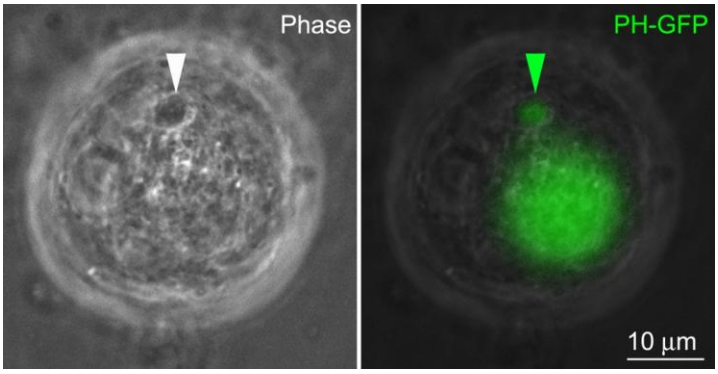

FIGURE 5. MDA-MB-231 cells were transfected with PH-GFP plasmid and placed in 3D culture. Arrows represent invadopodia.

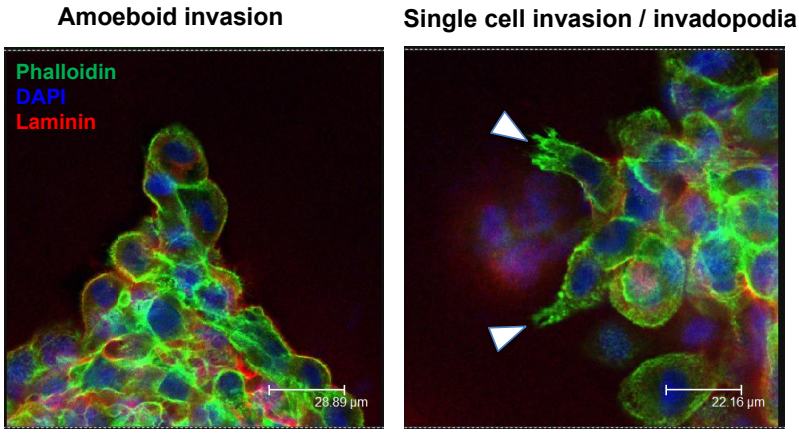

FIGURE 6. Radiation induces amoeboid and invadopia protrusions in ErbB2-overexpressing cells cultured in 3D conditions. MCF 10A-ErbB2 cells were treated with 2Gy X-rays. All images taken 14 days post-irradiation. Green corresponds to actin, red corresponds to laminin and blue corresponds to DAPI in confocal images. Arrows represent invadopodia formation.

Research Project 10: Project Title and Purpose

Using Biowalls to Sustainably Reduce Human Exposure to Indoor Volatile Organic Compounds - Exposure to Volatile Organic Compounds (VOCs) has been associated with health effects that include cancer, as well as respiratory, immunological, neurological, and renal effects. This study centers on the future Drexel Biowall, an indoor, vertical wall of plants designed to remove VOCs from the indoor air by using the bio-degrading capacity of microbes that live around the plant roots. The purpose of this work is to measure the VOC removal kinetics of microbial communities on plant roots for a common suite of eight VOCs at typical indoor concentrations while simultaneously characterizing the diversity, species, and numbers of bacteria in those root communities with both culture-independent and culture-dependent techniques. This work will allow us to identify efficient VOC degraders and clear a path for research bent on engineering effective degraders.

Anticipated Duration of Project

1/1/2011 - 12/31/2012

Project Overview

The broad research objective is to understand whether VOC removal by plant roots is a function of the diversity, species, and/or numbers of bacteria in those root communities. Aims 1 and 2 relate to developing the testing apparatus and measurement techniques required to fulfill this broad research objective:

(1) Construct the chamber system used to measure VOC removal by plant roots; and

(2) Develop culture-independent and culture-dependent methods to characterize diversity, species, and numbers of VOC degrading bacteria in plant root communities.

Once the apparatus and methods to characterize bacteria are developed, we will carry out Aims 3 and 4:

(3) Measure the VOC removal kinetics by microbial communities on roots of 12 plants for a common suite of eight VOCs at indoor concentrations typical of a new academic building over 22 weeks; and
(4) Periodically use culture-independent *and* culture-dependent techniques to characterize the diversity, species, and numbers of bacteria in those root communities over the 22 weeks of testing.

The chamber system will consist of individual growth vessels for each plant, which are grown aeroponically. Into each growth vessel, air containing particular concentrations of VOCs will be steadily delivered, and the removal for each VOC by each root system will be measured with a gas chromatograph/photo-ionization detector. On the same day as the VOC removal testing, we will characterize bacteria on those roots with: (a) Terminal Restriction Fragment Length Polymorphism (T-RFLP) to study changes in the diversity and composition of microbial communities among plant roots exposed to the VOCs; (b) High throughput 454 sequencing of bacterial 16S rRNA (targeting the V1-V3 regions) to identify the species found in the roots of plants that degrade VOCs; and (c) Real-time, quantitative PCR (qPCR) to estimate the numbers of bacteria on plant roots. To determine whether VOC degrading bacteria will increase in abundance after prolonged exposure to the VOC mixture (which should consequently increase the VOC removal rates over the 22 weeks of testing), we will compare the identity of bacteria that proliferate on roots after VOC exposure with the identity of bacteria cultivated from those plant roots and characterized *in vitro* with respect to their degradation capacities. That is, we will compare root bacteria that increase in abundance to those cultivated on media consisting of the VOC as the sole carbon source (e.g., benzoate as a mimic for benzene).

Principal Investigator

Michael S. Waring, PhD
Assistant Professor
Drexel University
Dept. of Civil, Architectural and Environmental Eng.
3141 Chestnut St. AEL 273-B
Philadelphia, PA 19104

Participating Researchers

Jacob A. Russell, PhD, Shivanthi Anandan, PhD - employed by Drexel University

Expected Research Outcomes and Benefits

Major outcomes of this work include: (1) Development of methods to be used to characterize VOC removal by roots of plants and to characterize bacterial diversity, species composition, and

number on plant roots. (2) A database of values of VOC removal kinetics as a function of bacterial diversity, species composition, and number of each type of species, for each VOC/plant combination. This database will be used to identify *associations* between the VOC removal and bacterial diversity, species composition, and number. Values in this database and these functional associations can be used in models we will develop in future work that predict VOC removal by Biowalls, which we can validate in the future Papadakis ISB (the building that will house the Drexel University Biowall). Once validated, these results can be used in VOC exposure models and risk analyses that elucidate the benefits of using Biowalls in institutional, academic, and corporate buildings, etc. Furthermore, it will be an important finding if bacterial communities are initially different on the plant roots but tend towards similar communities over time, which would imply that the types of plants present on the Biowall are much less important than the communities they harbor. Finally, identifying efficient VOC degraders will clear a path for research that attempts to engineer effective VOC-degrading bacteria for selective inoculation onto Biowalls; this inoculation will allow us to engineer Biowalls tailored to remove VOCs in particular buildings that have their own unique concentrations of health-degrading pollutants.

Summary of Research Completed

The work up to this point has been focused on completing Aims 1 and 2, which were (Aim 1) to construct the chamber system used to measure VOC removal by plant roots; and (Aim 2) to develop culture-independent and culture-dependent methods to characterize diversity, species, and numbers of VOC degrading bacteria in plant root communities. Both of these Aims contribute directly to the Expected Research Outcome 1, which is the development of methods to be used to characterize VOC removal by microbial root communities and to characterize bacterial diversity, species composition, and number on plant roots.

Regarding Aim 1, the construction of the apparatus to house the plants and allow the VOC removal testing has begun, and Figure 1 shows a schematic representation of the experimental system that we are constructing. In the center of the figure are four chambers. Each chamber is capable of aeroponically growing eight plants at one time. Two chambers serve as control chambers (A and B), and two serve as VOC-challenging chambers (C and D). VOC chambers will be exposed to VOCs during the entire 22 weeks of testing, while control chambers will only be exposed to VOCs during removal tests (which are each week). Chambers A and C will each house eight plants of the same species, and Chambers B and D will each house eight plants of a different species. For the VOC-challenging chambers, eight VOCs can be added with individual diffusion vessels (on left-hand side of the figure), whose delivery rates are controlled by the temperature of a digitally controlled oven. This way a range of concentrations of VOCs can be delivered to the aeroponic chambers. The gas-chromatograph/ flame ionization detector (GC/FID) has been ordered, and it will allow us to sample for VOC concentrations at various points in the experimental system, which will allow us to calculate our removal parameters when we conduct Aim 3 in future work. We are currently experimenting with different plant species to determine which ones grow well in our aeroponic system.

Regarding Aim 2, we have undertaken a series of investigations into cultivation-dependent and -independent methods for studies of microbes. Both approaches have been optimized and have yielded interesting results that show promise regarding future work with Aim 4.

Cultivation-independent approaches. At the start of this research, we first attempted to identify the most optimal method for extraction of DNA from plant roots, finding that the FastDNA soil kit gave the highest quality extractions as assessed through PCR reactions. With quality DNA in hand, we have proceeded to explore bacterial communities through the use of either restriction digests and fragment sizing or sequencing of products amplified with universal bacterial primers.

In all cases, the universal bacterial primers 9Fa and 1513R have proven to consistently amplify DNA from plant roots. And although no working primer set is truly universal, this pair has been shown to have a very broad applicability across the Eubacteria. A modified version of the former primer, with an attached fluorophore, was ordered and utilized for an approach known as T-RFLP (Terminal Restriction Fragment Length Polymorphism), in which amplified PCR products are digested with a sequence-specific enzyme, and then run on an automated sequencer to assess the size of the terminal fragment (i.e., the one containing the fluorophore-modified primer). Different bacteria will typically have different terminal fragment sizes, allowing us to examine and compare communities of these organisms within and between plants. As shown in Figure 2, the enzyme Bsh1236I generated over 30 fragments from PCR pools of two biowall grown plants—*Schefflera arboricola* and *Peperomia variegata*. This indicates that the root communities are fairly diverse, and that there are likely over two dozen common bacterial species on the roots of each of these plants when grown in a biowall (in this case, one at the Dodge Foundation in Morristown, NJ). It is also clear that plants share some bacterial types, which tells us that future attempts to inoculate multiple biowall grown plant species with selected VOC degraders could meet with some success.

Future studies of our root communities will employ the developed T-RFLP methodologies. We envision that these will give us a fast and affordable means to detect shifts in bacterial abundance over time in response to the VOC challenges outlined in our proposal.

To better identify the types of bacteria found on the roots, and to sample them in greater depth, we have begun to utilize 454 amplicon sequencing of 16S rRNA genes. Again, this approach involves the use of universal bacterial primers, which amplify a portion of this gene. Amplified pools of this gene (from a single root extraction) are then used as templates to generate 1,000-3,000 sequence reads per sample. Results from this approach are shown in Figure 3, which illustrates the abundance of different bacterial taxa from the roots of biowall grown plants. These results indicate that most bacteria from biowall grown plants come from one of ten abundantly represented orders. Yet the abundance of these orders may vary between plants—a possibility that will be examined further as we add replication within plants and within plant species.

Culture-dependent approaches. While a metagenomic (or metatranscriptomic) approach could eventually be used to study *in vivo* VOC degradation (and its mechanisms) by root communities, a more accessible approach involves cultivation of bacteria and subsequent characterization. Indeed, many root- and soil-associated bacteria are known to be cultivable, and this includes a number of VOC-degraders. And ultimately, genetic engineering and inoculation approaches will need to focus largely on cultivable bacteria, even if some VOC-degraders cannot be grown outside of roots. To begin characterizing the microbes present on plant roots, we have plated material from macerated (and surface-sterilized) root tissue on nutrient agar as well as sodium

benzoate media, which provides a benzene mimic as the sole carbon source. Both approaches have netted a variety of successfully cultivated microbial morphotypes, but the latter procedure has been given more attention, since it likely selects for degraders of a harmful VOC. Close-ups of a fungal and bacterial morphotype grown on benzoate are shown in Figure 4.

In Table 1, findings from PCR screens with bacterial and fungal primers (on DNA from the cultivated microbes), along with BLAST results, are illustrated. One result that is immediately clear is that most of the cultivated microbes were fungal in nature. Yet many of the fungi that formed distinct colonies on our plates appeared to be associated with bacteria—possible endo- or ecto-symbionts of the fungi. We have attempted to grow bacteria separately from fungi by cultivation on sodium benzoate plates with cyclohexamide. Yet few microbes grew at all under these conditions. Combined, these findings indicate that our future attempts to study VOC (especially benzene) degradation should eventually examine fungal communities (though the tools to do so are currently more limited than those for bacteria). But the bottom line is that this work has identified microbes that are indeed likely to degrade benzene. These can eventually be characterized and considered for inoculation experiments.

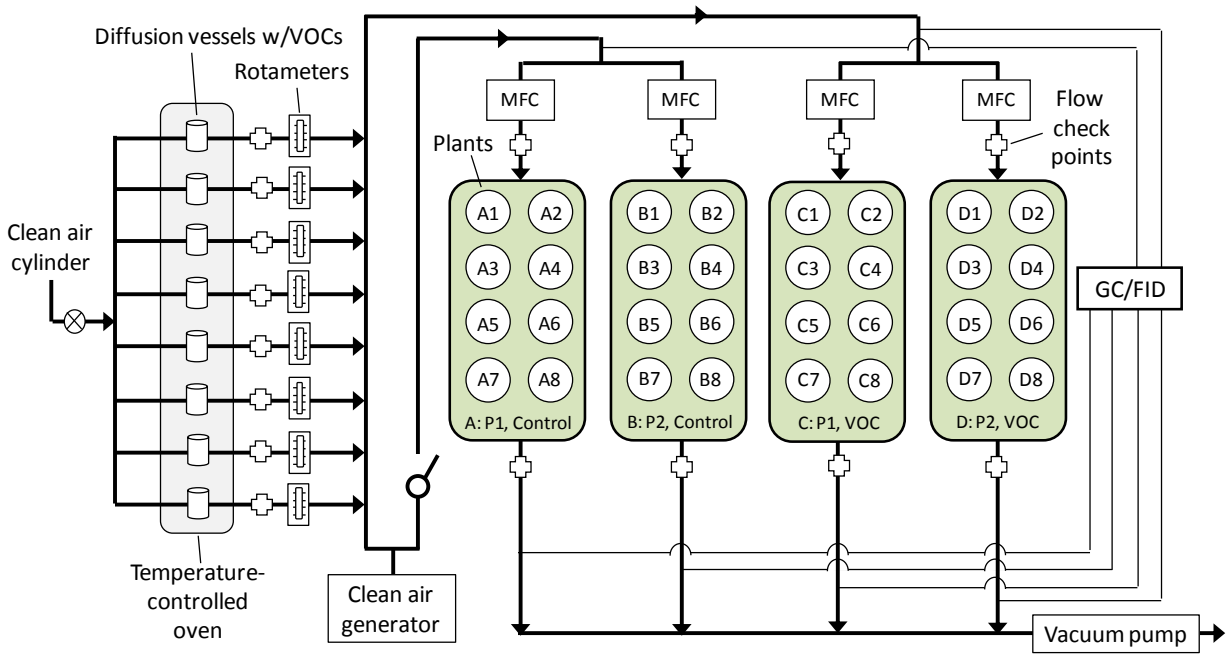

Figure 1. Schematic of the plant rearing and VOC removal testing apparatus being constructed. Eight plants will be grown aeroponically in each of the four chambers (A to D) in the middle of the schematic. MFC = mass flow controller.

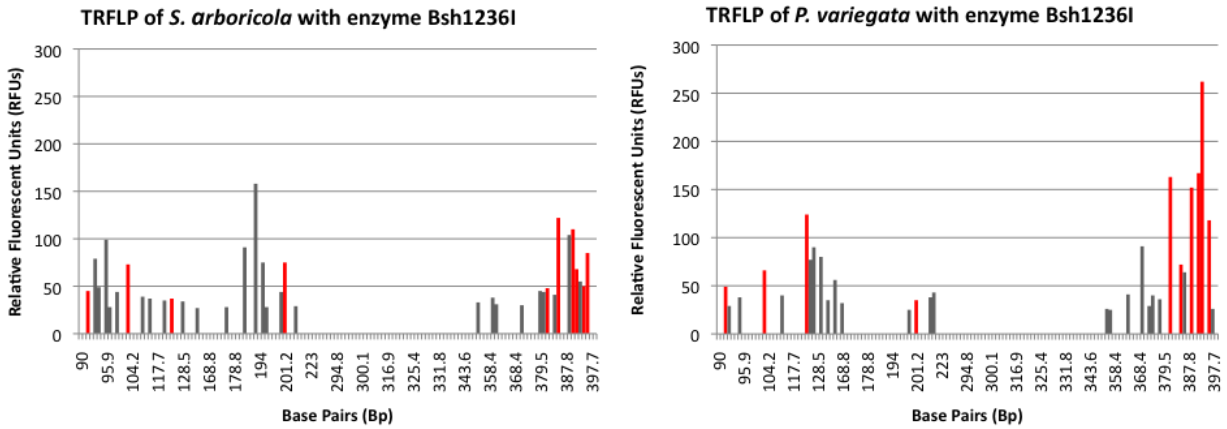

Figure 2. T-RFLP results of 16S rRNA genes amplified from root-associated bacteria of biowall grown plants. Fragment size is indicated on the x-axis, while abundance is illustrated on the y-axis. The enzyme Bsh1236I was used to cut universal PCR products from the roots of *Schefflera abrboricola* (left) and *Peperomia variegata* (right) which were grown in the Dodge Foundation biowall. Red bars reveal bacterial fragment sizes that were shared between the two plants.

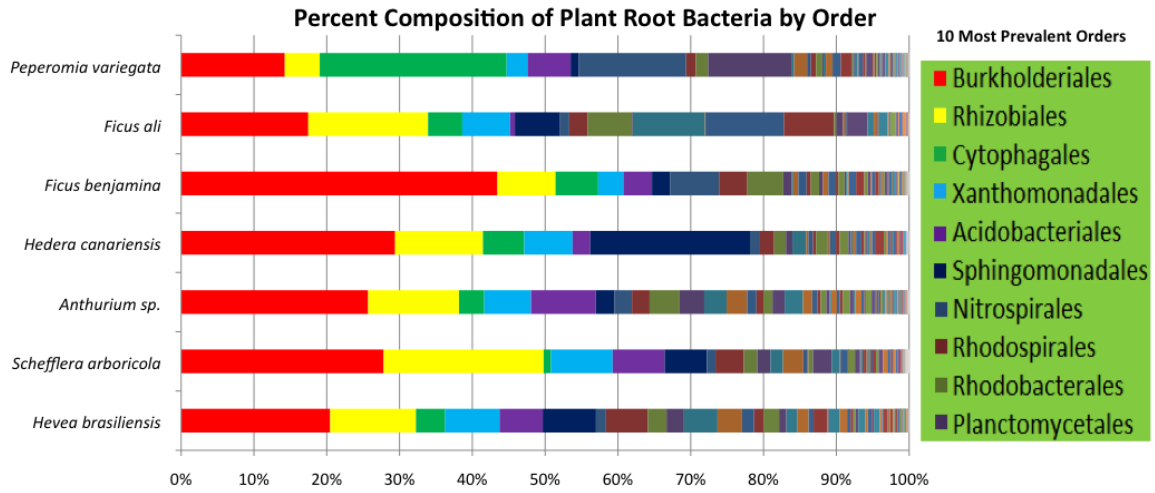

Figure 3. Taxonomic composition of bacteria from the roots of biowall grown plants. Microbes were sampled using high throughput 454 amplicon sequencing of 16S rRNA genes amplified with universal primers. Sequences (n>1,000 per sample) were then classified to bacterial orders for this analysis.

Figure 4. Microbial morphotypes cultivated on sodium benzoate media from the roots of biowall grown plants. The morphotype on the upper right corresponded to a fungus related to *Penicillium chrysogenum*, which was isolated from the roots of *Hedera canariensis* (upper left). The morphotype on the lower right belonged to a bacterium that was closely related to *Pseudomonas stutzeri*, originally isolated from the roots of *Schefflera arboricola*.

Table 1. BLAST hits of rRNA sequences from microbes cultivated on sodium benzoate.

Plant	**Morphotype #**	**Top Bacterial BLAST Hit (% identity)**	**Top Fungal BLAST Hit (% identity)**
H. brasiliensis	1	-	*Graphium fructicola* (98%)
S. arboricola	3	-	*Fusarium sp.* 18014 (97%)
	4	-	*Graphium fructicola* (98%)
	5	*Pseudomonas stutzeri* (98%)	*Fusarium sp.* 18014 (99%)
Anthurium sp.	6	-	*Fusarium oxysporum* (98%)
	7	*Staphylococcus sp.* (99%)	*Fusarium oxysporum* (98%)
	8	*Staphylococcus sp.* (98%)	*
H. canariensis	9	*Bacillus sp.* (99%)	*Penicillium chrysogenum* (99%)
	10	-	*Graphium fructicola* (98%)
	11	-	*Arthopyreniaceae sp.* (99%)
F. benjamina	12	-	*Fusarium sp.* 19001 (98%)
	13	*Staphylococcus sp.* (93%)	*Fusarium oxysporum* (98%)
	14	*Bacillus sp.* (99%)	*Fusarium sp.* 14018 (96%)
	15	*Staphylococcus sp.* (99%)	*Graphium fructicola* (99%)
F. ali	16	*Staphylococcus sp.* (98%)	*Orbilia delicatula* (78%)
	17	-	*Graphium fructicola* (97%)
P. variegata	18	*Bacillus sp.* (98%)	-
	19	-	*Penicillium camemberti* (98%)
	20	-	*Fusarium oxysporum* (99%)
	21	-	*Graphium fructicola* (99%)

* indicates that no quality DNA sequence was obtained in spite of a PCR positive.
- indicates that the PCR screen with either "universal" bacterial or fungal primers was negative.